Divergence in hormone signalling links local adaptation and hybrid failure

Melanie J. Wilkinson[1†], Federico Roda[1,2†], Greg M. Walter[1,3], Maddie E. James[1], Rick Nipper[4], Jessica Walsh[4], Scott L. Allen[1,5], Diana M. Bernal[1], Henry L. North[1,6], Christine A. Beveridge[1] and Daniel Ortiz-Barrientos[1*].

[1]The University of Queensland, School of Biological Sciences, St Lucia QLD 4072, Australia. [2]Current address: Universidad Nacional de Colombia, Departamento de Biología, Bogotá, Colombia. [3]Current address: University of Bristol, School of Biological Sciences, Senate House, Tyndall Ave, Bristol BS8 1TH, UK. [4]Floragenex, Inc., 4640 SW Macadam Avenue, Suite 200F, Portland, OR 97239, USA. [5]Current address: Institut für Populationsgenetik, Vetmeduni Vienna, Veterinärplatz 1, 1210, Wien, Austria. [6]Current address: University of Cambridge, Department of Zoology, Downing St., Cambridge CB2 3EJ, UK.

* Author for correspondence: Daniel Ortiz-Barrientos (*d.ortizbarrientos@uq.edu.au*)

† These authors contributed equally to the paper.

Abstract

Natural selection is a major driver for the origins of adaptations and new species[1]. Whether or not the processes driving adaptation and speciation share a molecular basis remains largely unknown[2]. Here, we show that divergence in hormone signalling contributed to the evolution of complex adaptations and intrinsic reproductive isolation in the Australian wildflower *Senecio lautus*. We provide evidence that differences in the auxin pathway, a hormone required for plant growth and development, has led to the repeated evolution of erect and prostrate forms along the Australian coast. Using multiple hybrid and natural populations, we show that adjacent erect and prostrate populations repeatedly diverged in auxin-related genes and auxin-dependent phenotypes, such as gravitropism. Analysis of a multi-year field selection experiment revealed that variation in fitness of an F10 hybrid population explained variation in gravitropism of their offspring. Genotyping of F11 hybrid individuals with extreme values of gravitropism revealed that variation in some of the most divergent genes explained both 65% of the variation in gravitropism and their probability of producing seed. Together, our results suggest that divergence in hormonal pathways can create a genetic link between rapid adaptation to new environments and the evolution of intrinsic reproductive isolation.

36 **Main text**

37 Ever since Darwin's work on the origin of new species by natural selection[1], a fundamental
38 question in evolutionary biology remains unanswered: Does adaptation and speciation share a
39 common genetic basis? Although several genes that cause hybrid failure, and therefore
40 impact speciation, have been identified[3], we still remain ignorant on whether genes driving
41 speciation have evolved as a by-product of local adaptation. One notable exception exists in
42 *Mimulus* populations adapted to copper mines where genetically linked loci for local
43 adaptation and hybrid mortality have been identified[4]. Here, we introduce a novel system and
44 a powerful way to uncover the molecular link between local adaptation and hybrid failure by
45 studying these processes in populations that have repeatedly and independently adapted to
46 contrasting environments. These highly replicated systems imply a role for natural selection
47 in the evolution of complex morphological or physiological differences[5,6], thus providing a
48 unique opportunity to examine if new species originate via the incidental evolution of
49 intrinsic barriers to reproduction between locally adapted populations.

50 We examine the genetics of repeated evolution of growth habit and its contribution to the
51 formation of intrinsic reproductive barriers between erect and prostrate populations of the
52 Australian wildflower, *Senecio lautus* (G.Forst. ex Willd)[7,8]. A previous population genetics
53 study in *S. lautus* found that sets of genes related by similar functions were repeatedly
54 differentiated in populations with these contrasting growth habits[9]. One of these sets
55 contained genes belonging to the auxin pathway, where genes involved in the polar transport
56 of this key plant hormone had repeatedly diverged between erect and prostrate populations.
57 Transport and regulation of auxin is required to create an auxin-concentration gradient that
58 alters the directional growth of a plant[10] and contributes to variation in height[11,12],
59 branching[13,14] and reproduction[15]. These traits distinguish the erect and prostrate growth

60 habits of *S. lautus* populations, therefore making evolution of the auxin pathway a natural
61 candidate to link the molecular basis of adaptation and speciation. We reasoned that if
62 divergence in the auxin pathway contributed to the evolution of adaptation and speciation in
63 *S. lautus*, we would discover the following evidence: First, we would detect similar patterns
64 of genetic divergence in auxin-related pathways across multiple erect and prostrate hybrid
65 and natural populations. Second, these populations would differ in phenotypes dependent on
66 auxin, such as their ability to alter the direction of growth in relation to gravity[10,16]. And third,
67 divergence in these auxin-dependent phenotypes would contribute to local adaptation and
68 intrinsic reproductive isolation between populations.

69 We test these hypotheses primarily on coastal populations of *S. lautus* (Fig. 1a, Extended
70 Data Table 1), which exhibit strong correlations between growth habit and the environments
71 they occupy[7]. Populations inhabiting sand dunes (Dune hereafter) are erect, while populations
72 growing on adjacent rocky headlands (Headland hereafter) are prostrate (Fig. 1b). Erect and
73 prostrate growth habits can also be found in related populations from the alpine regions of
74 Australia, with a prostrate population inhabiting an exposed alpine meadow and an erect
75 population inhabiting a sheltered alpine gully (Fig. 1c). Dune populations are continually
76 exposed to high temperatures and sun radiation, low salinity, and low nutrient sand substrate,
77 whereas Headland populations are exposed to high salinity, high nutrients and powerful
78 winds[17]. Neighbouring Dune and Headland populations are often sister taxa, group into two
79 major monophyletic clades (eastern and south-eastern) and have evolved their contrasting
80 growth habits independently multiple times[7,20]. These Dune and Headland populations are
81 locally adapted[17-20] and their F2 hybrids have low fitness[21], indicating the presence of
82 intrinsic reproductive isolation. Furthermore, performing genetic, physiological, and
83 ecological experimental studies is achievable in this system due to its short life cycle, diploid
84 inheritance, and small vegetative size. Therefore, the *Senecio lautus* species complex

85 provides an excellent system to understand the shared molecular basis of adaptation and
86 intrinsic reproductive isolation.

87 **Repeated evolution of auxin-related genes in *S. lautus***

88 To investigate whether there are similar patterns of genetic divergence in auxin-related
89 pathways across erect and prostrate populations, we assessed the genes that govern variation
90 in three traits that distinguish growth habit in *S. lautus* (plant vegetative height, main stem
91 angle and the number of tertiary branches; Extended Data Fig. 1). We performed a Bulk
92 Segregant Analysis (BSA)[22]. Briefly, we pooled individuals from the tails of each of the three
93 trait distributions and created reduced representation libraries for Genotyping-by-Sequencing.
94 BSA was performed in four independent mapping populations that represent replicates for the
95 evolution of the erect and prostrate morphologies in *S. lautus*[23] (Extended Data Fig. 2). In
96 agreement with a previous study in *S. lautus*[9], we found that highly differentiated genomic
97 regions (candidates) between extreme forms were often not the same across mapping
98 populations (Supplementary Table 1). Only 20 candidate regions were shared across all four
99 mapping populations: 14 candidates (out of 2,648) for main stem angle, six candidates for
100 branch number (out of 1,782) and zero candidates for height (out of 1,198), suggesting
101 repeated evolution at the gene level is limited. However, we found that 11 out of these 20
102 candidate regions contained genes regulating the auxin pathway (Extended Data Table 2),
103 implying evolution might have repeatedly occurred in hormone signalling pathways. Four of
104 these 11 genomic regions contained multiple auxin-related genes, which could indicate the
105 existence of pleiotropy or clusters of genes controlling variation in multiple adaptive traits.

106 Auxin candidate genes from the BSA also showed footprints of natural selection such as
107 genetic differentiation between adjacent populations, and/or significant associations with
108 survivorship in reciprocal transplants (Extended Data Table 2 and Supplementary Table 1).

109 This suggests that the auxin pathway might be important for adaptation to sand dunes and
110 rocky headlands. Several of these auxin genes also displayed differential expression between
111 shoot apical meristems of erect and prostrate populations (Extended Data Fig. 3), providing
112 further evidence for their involvement in mediating plant architecture differences. The
113 homologs of BSA candidate genes which participate in different steps of the auxin pathway,
114 include genes involved in auxin biosynthesis, gene expression regulation, and protein
115 modification. A large number of *S. lautus* scaffolds (28) were involved in intracellular auxin
116 transport (Extended Data Table 2), an essential process for creating auxin gradients that drive
117 a directional growth response to environmental cues such as light (phototropism) or gravity
118 (gravitropism)[16,24]. The homologs of some of these genes control gravitropism, apical
119 dominance, stem elongation and branching[10,13,14,16,25,26] (Extended Data Table 2), suggesting
120 that auxin-dependent phenotypes should be divergent between Dune and Headland
121 populations. Some homologs also have pleiotropic effects on reproduction (Extended Data
122 Table 2), which is consistent with a previous mapping experiment where quantitative trait
123 loci (QTL) were the same for plant architecture and hybrid fecundity between ecotypes of *S.*
124 *lautus*[27], indicating that we should also explore a genetic link between complex adaptations
125 and reproductive barriers between genetically and morphologically divergent populations.

126 **The physiological basis of repeated evolution in *S. lautus***

127 Considering we identified a multitude of different auxin related genes between erect and
128 prostrate populations of *S. lautus* and the regulation and transport of auxin is well established
129 to modulate gravitropism in plants, we predicted that these divergent growth habits may be a
130 direct consequence of changes in the auxin pathway, and can therefore contribute to
131 determining whether many plant species are erect or prostrate[26,28]. If this is true in *S. lautus*
132 then we would expect that gravitropism will predict plant height across populations, and that
133 differences in gravitropism will have occurred repeatedly between locally adapted

134 populations with contrasting morphologies. Finally, synthetic auxin and auxin transport
135 inhibitors will influence gravitropism differently between these erect and prostrate
136 populations.

137 To test whether gravitropism predicts plant height across populations, we first quantified
138 gravitropism and plant height in 16 *S. lautus* populations (Fig. 1 and Extended Data Fig. 4).
139 We defined the gravitropic response as the change in angle of a seedlings stem 24 hours after
140 a 90° rotation[29,30], where 0° is no gravitropic response and 90° is a complete re-orientation in
141 relation to the new gravity vector. If the auxin pathway has evolved differently between erect
142 and prostrate forms, we expect that prostrate populations will display a smaller gravitropic
143 angle than their adjacent erect population. Firstly, to show that height has a genetic basis in *S.*
144 *lautus* we confirmed that plant height in natural environments (field) and plant height in
145 common garden conditions (glasshouse) were strongly correlated ($F_{1,9}$=12.41, p=0.0065).
146 Next, we found that the average height of a population predicted its average gravitropic angle
147 (Fig. 2a; $F_{1,13}$=17.65, p=0.0010), where the average magnitude of gravitropism differed
148 between the two monophyletic clades ($F_{1,13}$=32.58, p<0.0001). These results suggest that
149 changes in gravitropism are genetically correlated with divergent growth habit traits such as
150 plant height, and that such correlation has evolved at least twice in the system. The strong
151 correlations between auxin-dependent phenotypes hint to an important role of natural
152 selection in the evolution of erect and prostrate forms.

153 To test whether differences in gravitropism will have occurred repeatedly between locally
154 adapted populations with contrasting morphologies, we compared gravitropism between
155 seven adjacent Dune and Headland population pairs (Extended Data Table 1). In four
156 population pairs the Headland population exhibited a smaller gravitropic angle and were
157 shorter than their adjacent Dune population (Fig. 2b, c). One population pair – Millicent –

158 also displayed a correlation between height and gravitropism, but where there was no
159 difference between the Dune and Headland populations for either trait (Fig. 2c), possibly due
160 to their similarity in environmental variables[23]. In two population pairs – Point Labatt and
161 Stradbroke Island – we did not observe the expected correlation between height and
162 gravitropism (Fig. 2b, c), suggesting that similar plant architectures could have evolved
163 through other developmental routes in coastal populations of *S. lautus*. We also assessed
164 height and gravitropism in divergent populations from the alpine region of Australia, and
165 discovered the expected pattern, where the exposed Alpine population in the meadow was
166 shorter and had a smaller gravitropic angle than the population in the sheltered Alpine gully
167 (Fig. 2c). These results provide additional evidence that divergent natural selection repeatedly
168 acting on auxin-dependent genes contribute to differences in gravitropism across coastal and
169 alpine populations in this system.

170 To directly test whether synthetic auxin and auxin transport inhibitors will influence
171 gravitropism differently between these erect and prostrate populations, we grew Lennox Head
172 Dune and Headland seeds with synthetic auxin, 2,4-Dichlorophenoxyacetic acid (2,4-D), and
173 polar auxin transport inhibitor, naphthylphthalamic acid (NPA)[31,32]. Because a gravitropic
174 response requires an auxin concentration gradient, we reasoned that removing the gradient
175 would reduce the gravitropic angle in Dune individuals (Extended Data Fig. 5). As expected,
176 addition of synthetic auxin 2,4-D reduced the gravitropic angle more in Dune individuals
177 (from 66.34±2.27° to 19.44±7.64°) than in Headland individuals (LR chi-square, X^2_2=18.49,
178 $p<0.0001$). Similarly, addition of auxin transport inhibitor NPA reduced the gravitropic angle
179 in our experiments more in Dune individuals (from 62.57±3.62° to 20.47±13.67°) than in
180 Headland individuals (LR chi-square, X^2_3=21.18, $p<0.0001$). This difference in hormone
181 response in Dune and Headland individuals supports our hypothesis that differences in the
182 auxin pathway underlie the different gravitropic responses in *S. lautus*.

183 Overall, these three results reveal that genetic differences in the auxin pathway have
184 contributed to the repeated evolution of growth habit in this system[23]. Moreover, our findings
185 support the hypothesis that natural selection may be the major evolutionary force responsible
186 for the physiological and morphological diversity underpinning the differences in growth
187 habit between Dune and Headland populations.

188 **Adaptive evolution of auxin-dependent phenotypes in *S. lautus***

189 Having established that auxin-related genes have diverged between erect and prostrate forms
190 in *S. lautus,* we conducted two independent sets of field experiments to experimentally assess
191 the role of natural selection on the evolution of classical auxin-dependent phenotypes, height
192 (height adaptation experiments) and gravitropism (gravitropism adaptation experiments). In
193 each field experiment, Dune and Headland parental and hybrid seeds were transplanted into
194 replicated blocks at the sand dune and rocky headland at Lennox Head. In all field
195 experiments, divergent natural selection consistently favoured the local Dune or Headland
196 population over the foreign population (Fig. 3), indicating that experimental conditions
197 captured local adaptation in both environments.

198 **Height adaptation experiments:** We tested whether differences in height could drive
199 differences in fitness in the rocky headlands. We hypothesised that offspring produced by
200 short hybrid parents would live longer than offspring produced by tall hybrid parents in the
201 rocky headland. We focused on prostrate growth as it is likely the derived trait because the
202 majority of populations in the *S. lautus* species complex have an erect growth habit[9,17]. We
203 introgressed Dune alleles associated with height onto a Headland genomic background.
204 Briefly, we crossed Lennox Head Dune and Headland parentals and then completed two
205 rounds of backcrossing followed by one round of crossing between tall hybrid offspring and
206 between short hybrid offspring (Extended Data Fig. 6). We transplanted 558 of these seeds

207 (from 28 families) into the rocky headland. As predicted shorter hybrid parents produced
208 offspring that lived longer in the rocky headland relative to offspring from taller hybrid
209 parents ($F_{1,26.23}$=4.87, p=0.0362). These results suggest that traits genetically correlated with
210 plant height contributed to early developmental fitness in the rocky headlands and contributed
211 directly or indirectly to the evolution of divergent growth habit.

212 **Gravitropism adaptation experiments:** We tested whether rapid adaptation to contrasting
213 environments can lead to the evolution of gravitropic responses in the direction of the local
214 population, and to the formation of a genetic correlation with plant height. We hypothesised
215 that exposing an advanced recombinant population to multiple rounds of viability selection in
216 the field would drive genetic covariation between fitness and gravitropism. To test this
217 hypothesis, we crossed the Dune and Headland populations from Lennox Head for eight
218 generations using recombination to disassemble allelic combinations and construct a
219 recombinant hybrid population[27] (Fig. 4a). We planted 2,403 of these F8 seeds (from 89
220 families) into the sand dune and rocky headland (Fig. 4b) and conducted family-based
221 truncation selection for three generations, planting a similar number of seeds and families in
222 the F9 and F10 generation (Extended Data Table 3). We selected the top 50% of surviving
223 families in each environment, and subsequently crossed their full-siblings in the glasshouse to
224 produce the next generation. In the F10 generation, we tested whether families that had the
225 greatest number of survivors also produced offspring with the local gravitropic response
226 under laboratory conditions. In agreement with our hypothesis, F10 families with the greatest
227 number of survivors in the sand dune produced offspring with a higher gravitropic angle
228 (Table 1). We discovered that the relationship between fitness of the F10 families in the sand
229 dune and the gravitropic response in the F11 generation in the glasshouse was dependent on
230 fitness of the F10 dam family (Table 1), suggesting maternal genotypes contribute to the
231 evolution of gravitropism in the sand dunes. On the other hand, all F10 families in the rocky

232 headland produced offspring with intermediate levels of gravitropism (Table 1). Notably, in
233 the F11 recombinant Control population that was grown and crossed in the glasshouse only,
234 height and gravitropism were not genetically correlated ($F_{1,114.3}$=0.08, p=0.7801, r^2=0.04), but
235 this genetic correlation was quickly regained after three rounds of selection in the rocky
236 headland ($F_{1,169.5}$=7.09, p=0.0085, r^2=0.27) and weakly regained in the sand dune
237 ($F_{1,151.3}$=3.20, p=0.0756, r^2=0.09). Together, these results suggest that natural selection can
238 act on standing genetic variation and reconstitute genetic architectures that favour a
239 correlation between survivorship and gravitropism in the environments where the coastal
240 populations are found.

241 Given the divergence in multiple auxin-dependent phenotypes between Dune and Headland
242 populations described throughout this paper, these results imply that natural selection of
243 hormonal pathways can aid in the rapid evolution of multiple integrated phenotypes when
244 encountering a new selection pressure.

245 **The genes underlying gravitropism in *S. lautus***

246 Having shown that natural selection drove the rapid evolution of gravitropism in *S. lautus*
247 under experimental conditions in the field, we can identify the genes underlying adaptation
248 by detecting extreme allelic differences between the F11 individuals with the smallest
249 gravitropic angle (agravitropic tail, <20°; mean of tail = 6.46±1.10°, n=68) and the largest
250 gravitropic angle (gravitropic tail, >56°; mean of tail = 62.03±0.45°, n=77). We performed
251 selective genotyping on these tails of the gravitropic distribution in the F11 recombinant
252 populations (Fig. 4c; Dune and Headland survivors, and Control individuals) and created a
253 gravitropism candidate gene set with allelic differences in the 99.9% quantile ($0.15<p<0.22$).
254 We identified 55 sites (0.2% of all SNPs) across 49 genomic scaffolds in this quantile
255 (Supplementary Table 2) and discovered that these genes disproportionally represented gene

256 ontology categories of transport and localisation of molecules across and between cells
257 (Extended Data Table 4).

258 Five of the 55 sites (11%) are located in gene homologs with functions related to the auxin
259 pathway, including the second (ENODL1/WAT1; Early nodulin-like protein 1/Walls are thin
260 1) and fourth (ABA3; molybdenum cofactor sulfurase) most differentiated SNPs between the
261 agravitropic and gravitropic F11 tails. In both ENODL1 and ABA3 genes, the allele
262 frequency of the F11 tails shifted in the direction of the most common allele in the native
263 population with the same phenotype. For instance, ENODL1 C allele and ABA3 G allele was
264 favoured in both the Headland population and agravitropic F11 tail, with the alternate alleles
265 being favoured in the Dune population and the gravitropic F11 tail. ENODL1 and ABA3
266 were in strong linkage disequilibrium in the survivors of the gravitropism adaptation
267 experiment in the rocky headland (Fisher's exact test, n=57, p=0.0008) and sand dune
268 (Fisher's exact test, n=48, p=0.0107), but not in the glasshouse (Fisher's exact test, n=37,
269 p=0.4093), suggesting natural selection has driven the evolution of this allelic combination.
270 ENODL1 C/C and ABA3 G/G genotypes were associated with a reduction in gravitropism of
271 25.10° relative to all other genotype combinations (Fig. 5; $t_{34.30}$=4.86, p<0.0001). Further, the
272 gravitropism distribution across all F11 individuals is bimodal with the agravitropic peak at
273 2.56° (95% CIs=1.17-3.95) and the gravitropic peak at 41.13° (95% CIs=39.85-42.40),
274 indicating that the ENODL1 C/C and ABA3 G/G genotype combination explains 65% of the
275 difference in gravitropism. Together, these results suggest that a small gravitropic angle is a
276 recessive phenotype, and that natural selection has targeted few genetic regions of large
277 effect. Whilst ENODL1 and ABA3 are not classical auxin genes, they have functions in
278 gravitropism, plant height, salt tolerance and pollen tube growth across different plant
279 species[33-39], and therefore are strong candidates to not only explain the adaptive evolution of
280 gravitropism, but other phenotypic differences between Dune and Headland populations.

281 Moreover, ENODL1 was also associated with field survivorship in a previous BSA study in
282 this system[27] and with height in one of the BSA populations we used here for genetic
283 mapping of convergent traits.

284 Overall, our results suggest that divergence in auxin-regulated molecular processes
285 contributed to local adaptation to contrasting environments in coastal populations of *S. lautus*.

286 **The consequences of gravitropism divergence on the evolution of intrinsic reproductive**
287 **isolation**

288 We are now in a unique position to address whether adaptation and speciation have a
289 common molecular basis. Specifically, we can test whether divergent gravitropic forms are
290 reproductively isolated. To assess this problem, we investigated the effects of gravitropism on
291 reproductive success in the F11 hybrids. We created two groups of crosses among F11
292 families: crosses within (agravitropic x agravitropic, n=28; gravitropic x gravitropic, n=37)
293 and crosses between (agravitropic x gravitropic, n=67) the tails of the gravitropic distribution.
294 We found that crosses failed more often between F11 agravitropic and gravitropic plants
295 (21%) than crosses within each of these tails (5%; Fisher's exact test, n=132, p=0.0079). Of
296 the 11 failed crosses with known genotypes, only one cross had the ENODL1 C/C genotype,
297 none had the ABA3 G/G genotype, and none were double homozygous for the two genes,
298 suggesting that evolution of a small gravitropic angle possibly relied on the recessive x
299 recessive interaction. These results imply a genetic link between adaptation and intrinsic
300 reproductive isolation among populations that occupy these contrasting environments.

301 **Discussion**

302 Here we have discovered that divergence in auxin-related pathways contribute to the repeated
303 evolution of growth habit in *S. lautus*, suggesting that evolution in hormone signalling could
304 facilitate colonisation of new habitats through concomitant changes in multiple

305 developmental and architectural traits. Consistent with our results, transitions from erect to
306 prostrate growth and the associated phenotypes of height, main stem angle and number of
307 branches, are common in plants that colonize coastal headlands[40-43]. This indicates that there
308 are strong selective agents common to headland environments. For example, powerful winds
309 or salty substrates could impose early selective pressure in traits controlled by auxins such as
310 responses to mechanical cues[44] and halotropism[45-47]. Further, we discovered that divergence
311 in growth habit was genetically correlated with intrinsic reproductive isolation in *S. lautus*,
312 implying that hormone signalling divergence might lead to pleiotropic evolution of genetic
313 incompatibilities that reduce hybrid fitness or pollen-pistil interactions (e.g., differences in
314 pollen tube growth[48]) that prevent fertilisation. Together, these results suggest that divergence
315 in plant hormonal pathways that affect multiple traits during plant development and
316 reproduction could be a powerful mechanism to link the genetic, ecological and physiological
317 basis of adaptation and speciation in plants.

318 The roles of hormone signalling in plant adaptation and intrinsic reproductive isolation have
319 been explored independently but only in rare cases have the two been linked. The hormonal
320 pathways most commonly involved in plant adaptation are the abscisic acid pathway, which
321 is involved in stress response[49], the jasmonate signalling that contributes to the growth-
322 defence conflict[50], and the auxin pathway that responds to salt tolerance[45-47] and mechanical
323 stress responses[44]. On the other hand, hormonal pathways involved in intrinsic reproductive
324 isolation include breakdown of cytokines in hybrid sterility[51], and the auxin pathway in
325 pollen tube growth[48]. In more recent work in *Arabidopsis*[52] and *Mimulus*[53], variation in genes
326 involved in the gibberellin pathway were associated with variation in both morphological
327 differentiation and local adaptation to different environments. The consequences of such
328 adaptation for the evolution of intrinsic reproductive isolation remain unclear, but at least in
329 *Mimulus*, many of the gibberellin genes associated with local adaptation reside within a

330 chromosomal inversion strongly associated with flowering time differences between coastal
331 and inland ecotypes[53,54]. Our study takes us a step further by directly linking natural selection
332 and divergence in hormone signalling with pleiotropic effects on intrinsic reproductive
333 isolation in a highly replicated system of evolution, thus paving the way to uncover the
334 molecular basis of repeated evolution and its consequences on the evolution of intrinsic
335 reproductive isolation in plants.

336 Overall, our study illustrates a powerful strategy to explore the genetic basis of adaptation in
337 natural systems that takes us away from a gene-centric paradigm and moves us towards
338 identifying sets of genes related by function. We conjecture that the evolution of hormonal
339 pathways in plants, provides a simple mechanism for the rapid origin of integrated
340 phenotypes that facilitate colonisation of new habitats, and to the incidental evolution of
341 intrinsic reproductive isolation as a consequence.

342 **Acknowledgements**

343 We are grateful to S. Smith, L.H. Rieseberg, M. Cooper, M.A.F. Noor and members of the
344 Ortiz-Barrientos laboratory for insightful comments on previous versions of this manuscript.
345 S. Karrenberg and S. Chenoweth provided very useful feedback on M.J. Wilkinson PhD
346 dissertation. We thank P. Brewer for his help in the design and execution of gravitropism
347 experiments, T. Richards for his contributions to the construction of recombinant populations
348 for BSA, and J. Donohoe for his help in the phenotyping and rearing of plants for BSA.

349 **Data archival**

350 **Author contributions**

351 MJW, FR, DO conceived the projects and experiments. MJW conducted height adaptation
352 experiments, reared and phenotyped various glasshouse populations and performed

353 reproductive isolation experiment. FR created BSA mapping populations and performed BSA
354 analyses. FR and MJW performed physiological and molecular biology experiments. GMW
355 reared and phenotyped the natural populations in the glasshouse and conducted the field
356 experiment for the gravitropism adaptation experiments with assistance from MJW, MEJ, FR
357 and DO. DMB performed expression analyses. MJW, MEJ and HN phenotyped natural
358 populations. RN and JW called the genotypes of the F11 population. SA assembled the
359 current draft genome of *S. lautus*. CB guided the physiological experiments. MJW, FR, DO
360 wrote the paper with input from all authors. DO is mentor and supervisor for the research
361 program.

362 **Conflicts of interest**

363 We do not have any conflicts of interest.

364 **References**

365 1 Darwin, C. *On the origins of species by means of natural selection*. Vol. 247 (1859).
366 2 Baack, E., Melo, M. C., Rieseberg, L. H. & Ortiz-Barrientos, D. The origins of reproductive
367 isolation in plants. *New Phytologist* **207**, 968-984, doi:10.1111/nph.13424 (2015).
368 3 Fishman, L. & Sweigart, A. L. When Two Rights Make a Wrong: The Evolutionary Genetics of
369 Plant Hybrid Incompatibilities. *Annual review of plant biology*, doi:10.1146/annurev-arplant-
370 042817-040113 (2018).
371 4 Wright, K. M., Lloyd, D., Lowry, D. B., Macnair, M. R. & Willis, J. H. Indirect evolution of
372 hybrid lethality due to linkage with selected locus in *Mimulus guttatus*. *PLOS Biology* **11**,
373 e1001497, doi:10.1371/journal.pbio.1001497 (2013).
374 5 Stinchcombe, J. R. & Hoekstra, H. E. Combining population genomics and quantitative
375 genetics: finding the genes underlying ecologically important traits. *Heredity* **100**, 158-170
376 (2007).
377 6 Barrett, R. D. H. & Schluter, D. Adaptation from standing genetic variation. *Trends in Ecology*
378 *& Evolution* **23**, 38-44, doi:10.1016/j.tree.2007.09.008 (2008).
379 7 Radford, I. J., Cousens, R. D. & Michael, P. W. Morphological and genetic variation in the
380 *Senecio pinnatifolius* complex: are variants worthy of taxonomic recognition? *Australian*
381 *Systematic Botany* **17**, 29-48, doi:10.1071/sb03013 (2004).
382 8 Thompson, I. *Taxonomic studies of Australian Senecio (Asteraceae): 5. The S. lautus/S. lautus*
383 *complex.*, 23-76 (Royal Botanic Gardens, 2005).
384 9 Roda, F. *et al.* Convergence and divergence during the adaptation to similar environments by
385 an Australian groundsel. *Evolution* **67**, 2515-2529, doi:10.1111/evo.12136 (2013).
386 10 Friml, J. Auxin transport—shaping the plant. *Current opinion in plant biology* **6**, 7-12 (2003).

11 Xu, M., Zhu, L., Shou, H. & Wu, P. A PIN1 family gene, OsPIN1, involved in auxin-dependent adventitious root emergence and tillering in rice. *Plant and Cell Physiology* **46**, 1674-1681, doi:10.1093/pcp/pci183 (2005).
12 Wallace, J. G. *et al.* Genome-wide association for plant height and flowering time across 15 tropical maize populations under managed drought stress and well-watered conditions in Sub-Saharan Africa. *Crop Science* **56**, 2365-2378, doi:10.2135/cropsci2015.10.0632 (2016).
13 Gallavotti, A. The role of auxin in shaping shoot architecture. *Journal of Experimental Botany* **64**, 2593-2608, doi:10.1093/jxb/ert141 (2013).
14 Domagalska, M. a. & Leyser, O. Signal integration in the control of shoot branching. *Nature Reviews Molecular Cell Biology* **12**, 211-221, doi:10.1038/nrm3088 (2011).
15 Sundberg, E. & Østergaard, L. Distinct and dynamic auxin activities during reproductive development. *Cold Spring Harbor perspectives in biology* **1**, a001628-a001628, doi:10.1101/cshperspect.a001628 (2009).
16 Vanneste, S. & Friml, J. Auxin: a trigger for change in plant development. *Cell* **136**, 1005-1016, doi:10.1016/j.cell.2009.03.001 (2009).
17 Walter, G. M. *et al.* Diversification across a heterogeneous landscape. *Evolution* **70**, 1979-1992, doi:10.1111/evo.13009 (2016).
18 Melo, M. C., Grealy, A., Brittain, B., Walter, G. M. & Ortiz-Barrientos, D. Strong extrinsic reproductive isolation between parapatric populations of an Australian groundsel. *New Phytologist* **203**, 323-334, doi:10.1111/nph.12779 (2014).
19 Richards, T. J. & Ortiz-Barrientos, D. Immigrant inviability produces a strong barrier to gene flow between parapatric ecotypes of *Senecio lautus*. *Evolution* **70**, 1239-1248, doi:10.1111/evo.12936 (2016).
20 Richards, T. J., Walter, G. M., McGuigan, K. & Ortiz-Barrientos, D. Divergent natural selection drives the evolution of reproductive isolation in an Australian wildflower. *Evolution* **70**, 1993-2003, doi:10.1111/evo.12994 (2016).
21 Walter, G. M., Aguirre, J. D., Blows, M. W. & Ortiz-Barrientos, D. Evolution of genetic variance during adaptive radiation. *The American Naturalist* **191**, E108-E128, doi:10.1086/696123 (2018).
22 Michelmore, R. W., Paran, I. & Kesseli, R. V. Identification of markers linked to disease-resistance genes by bulked segregant analysis: a rapid method to detect markers in specific genomic regions by using segregating populations. *Proceedings of the National Academy of Sciences* **88**, 9828-9832, doi:10.1073/pnas.88.21.9828 (1991).
23 Roda, F. *et al.* Genomic evidence for the parallel evolution of coastal forms in the *Senecio lautus* complex. *Molecular Ecology* **22**, 2941-2952, doi:10.1111/mec.12311 (2013).
24 Petrasek, J. & Friml, J. Auxin transport routes in plant development. *Development* **136**, 2675-2688, doi:10.1242/dev.030353 (2009).
25 Dun, E. A., Ferguson, B. J. & Beveridge, C. A. Apical dominance and shoot branching. Divergent opinions or divergent mechanisms? *Plant Physiology* **142**, 812-819 (2006).
26 Li, P. *et al.* LAZY1 controls rice shoot gravitropism through regulating polar auxin transport. *Cell Research* **17**, 402-410, doi:10.1038/cr.2007.38 (2007).
27 Roda, F., Walter, G. M., Nipper, R. & Ortiz-Barrientos, D. Genomic clustering of adaptive loci during parallel evolution of an Australian wildflower. *Molecular Ecology* **26**, 3687–3699, doi:10.1111/mec.14150 (2017).
28 Tan, L. *et al.* Control of a key transition from prostrate to erect growth in rice domestication. *Nature genetics* **40**, 1360-1364, doi:10.1038/ng.197 (2008).
29 Lopez, D., Tocquard, K., Venisse, J.-S., Legué, V. & Roeckel-Drevet, P. Gravity sensing, a largely misunderstood trigger of plant orientated growth. *Frontiers in Plant Science* **5**, doi:10.3389/fpls.2014.00610 (2014).
30 Blancaflor, E. B. Regulation of plant gravity sensing and signaling by the actin cytoskeleton. *American Journal of Botany* **100**, 143-152, doi:10.3732/ajb.1200283 (2013).

31 Yamamoto, M. & Yamamoto, K. T. Differential effects of 1-naphthaleneacetic acid, indole-3-acetic acid and 2,4-dichlorophenoxyacetic acid on the gravitropic response of roots in an auxin-resistant mutant of *Arabidopsis*, *auxl*. *Plant and Cell Physiology* **39**, 660-664 (1998).

32 Ottenschläger, I. *et al.* Gravity-regulated differential auxin transport from columella to lateral root cap cells. *Proceedings of the National Academy of Sciences* **100**, 2987-2991, doi:10.1073/pnas.0437936100 (2003).

33 Ranocha, P. *et al.* Walls are thin 1 (WAT1), an *Arabidopsis* homolog of *Medicago truncatula* NODULIN21, is a tonoplast-localized protein required for secondary wall formation in fibers. *The Plant Journal* **63**, 469-483, doi:10.1111/j.1365-313X.2010.04256.x (2010).

34 Promchuea, S., Zhu, Y., Chen, Z., Zhang, J. & Gong, Z. ARF2 coordinates with PLETHORAs and PINs to orchestrate ABA-mediated root meristem activity in *Arabidopsis*. *Journal of integrative plant biology* **59**, 30-43, doi:10.1111/jipb.12506 (2017).

35 Wu, H., Shen, Y., Hu, Y., Tan, S. & Lin, Z. A phytocyanin-related early nodulin-like gene, BcBCP1, cloned from *Boea crassifolia* enhances osmotic tolerance in transgenic tobacco. *Journal of Plant Physiology* **168**, 935-943, doi:10.1016/j.jplph.2010.09.019 (2011).

36 Ma, H., Zhao, H., Liu, Z. & Zhao, J. The phytocyanin gene family in rice (Oryza sativa L.): Genome-wide identification, classification and transcriptional analysis. *PLOS ONE* **6**, e25184, doi:10.1371/journal.pone.0025184 (2011).

37 Garcia de la Garma, J. *et al.* New insights into plant salt acclimation: the roles of vesicle trafficking and reactive oxygen species signalling in mitochondria and the endomembrane system. *New Phytologist* **205**, 216-239, doi:10.1111/nph.12997 (2015).

38 Mittler, R. & Blumwald, E. The roles of ROS and ABA in systemic acquired acclimation. *The Plant Cell* **27**, 64-70 (2015).

39 Hou, Y. *et al.* Maternal ENODLs are required for pollen tube reception in *Arabidopsis*. *Current Biology* **26**, 2343-2350, doi:10.1016/j.cub.2016.06.053 (2016).

40 Beeftink, W., Rozema, J. & Huiskes, A. *Ecology of coastal vegetation*. Vol. 6 (Springer, 1985).

41 Auld, T. & Morrison, D. Genetic determination of erect and prostrate growth habit in five shrubs from windswept headlands in the Sydney region. *Australian Journal of Botany* **40**, 1-11 (1992).

42 Morrison, D. & Rupp, A. Patterns of morphological variation within Acacia suaveolens (Mimosaceae). *Australian Systematic Botany*, 1013-1027 (1995).

43 Crutsinger, G. M., Strauss, S. Y. & Rudgers, J. a. Genetic variation within a dominant shrub species determines plant species colonization in a coastal dune ecosystem. *Ecology* **91**, 1237-1243 (2010).

44 Li, T. *et al.* Calcium signals are necessary to establish auxin transporter polarity in a plant stem cell niche. *Nature Communications* **10**, 726, doi:10.1038/s41467-019-08575-6 (2019).

45 Naser, V. & Shani, E. Auxin response under osmotic stress. *Plant molecular biology* **91**, 661-672, doi:10.1007/s11103-016-0476-5 (2016).

46 van den Berg, T., Korver, R. A., Testerink, C. & ten Tusscher, K. H. Modeling halotropism: a key role for root tip architecture and reflux loop remodeling in redistributing auxin. *Development* **143**, 3350-3362 (2016).

47 Galvan-Ampudia, C. S. *et al.* Halotropism is a response of plant roots to avoid a saline environment. *Current Biology* **23**, 2044-2050 (2013).

48 Guan, Y., Guo, J., Li, H. & Yang, Z. Signaling in Pollen Tube Growth: Crosstalk, Feedback, and Missing Links. *Molecular Plant* **6**, 1053-1064, doi:10.1093/mp/sst070 (2013).

49 Tuteja, N. Abscisic Acid and Abiotic Stress Signaling. *Plant signaling & behavior* **2**, 135-138, doi:10.4161/psb.2.3.4156 (2007).

50 Guo, Q., Major, I. T. & Howe, G. A. Resolution of growth-defense conflict: mechanistic insights from jasmonate signaling. *Curr Opin Plant Biol* **44**, 72-81, doi:10.1016/j.pbi.2018.02.009 (2018).

51 Bomblies, K. & Weigel, D. Hybrid necrosis: autoimmunity as a potential gene-flow barrier in plant species. *Nature Reviews Genetics* **8**, 382, doi:10.1038/nrg2082 (2007).

52 Luo, Y. *et al.* A Single Nucleotide Deletion in *Gibberellin20-oxidase1* Causes Alpine Dwarfism in Arabidopsis. *Plant Physiology* **168**, 930, doi:10.1104/pp.15.00005 (2015).

53 Gould, B. A., Chen, Y. & Lowry, D. B. Pooled ecotype sequencing reveals candidate genetic mechanisms for adaptive differentiation and reproductive isolation. *Molecular Ecology* **26**, 163-177, doi:10.1111/mec.13881 (2017).

54 Lowry, D. B. & Willis, J. H. A widespread chromosomal inversion polymorphism contributes to a major life-history transition, local adaptation, and reproductive isolation. *PLOS Biology* **8**, e1000500, doi:10.1371/journal.pbio.1000500 (2010).

Figures and Tables

Table 1. General linear model for the effect of dam and sire on gravitropism (°) after a field selection experiment on a recombinant hybrid Dune and Headland population.

	Dune				Headland			
Source	DF	SS	F-Ratio	Prob > F	DF	SS	F-Ratio	Prob > F
Dam family fitness	6	8515.77	4.779	<0.001	6	1884.31	0.701	0.650
Sire family fitness	6	1806.62	1.014	0.424	5	2315.36	1.033	0.405
Intrinsic viability	1	260.85	0.878	0.352	1	5209.38	11.624	0.001
Genetic replicate	3	1135.49	1.275	0.290	3	3357.19	2.497	0.067
Temporal block	2	193.14	0.325	0.724	2	2234.96	2.494	0.090

DF, degrees of freedom; SS, sum of squares.

Field selection experiments were performed on F8, F9 and F10 recombinant hybrid generations to achieve three rounds of selection in the sand dune and rocky headland at Lennox Head (see Fig. 4 for the experimental design). Dam and sire fitness are the F10 family fitness values for the individuals that were crossed to create the F11 offspring where gravitropism was measured. Intrinsic viability is the number of days until death of the F11 generation in the controlled temperature room. This experiment was conducted three times (temporal block) with three independent genetic replicates.

Fig. 1: Growth habit differences between *S. lautus* ecotypes that grow adjacently across south-east Australia.

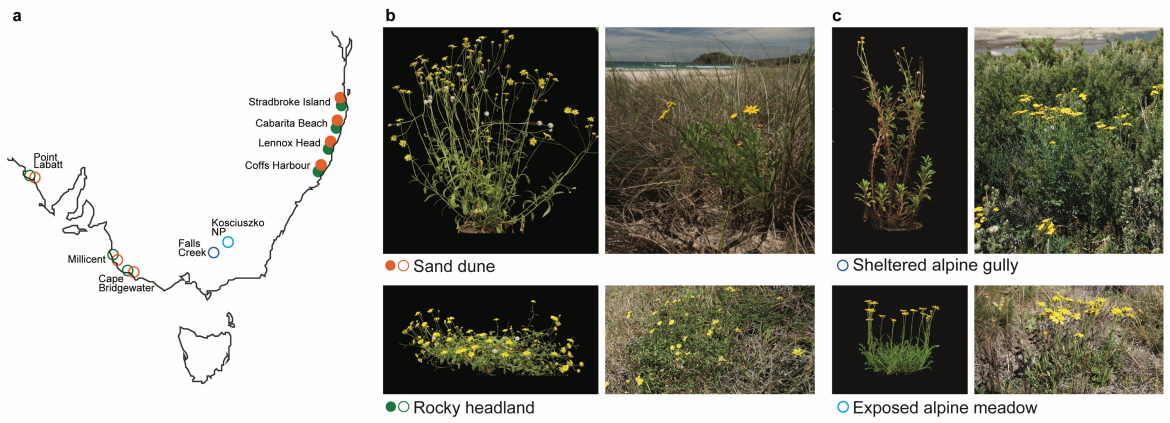

a, Map of Australia showing locations of the 16 populations used in this study. The seven coastal localities have a Dune (orange) and Headland (green) population occurring adjacent to each other. The populations are split into two monophyletic clades[23], the eastern clade (closed circles) and the south-eastern clade (open circles). **b,** *Senecio lautus* native to the sand dunes have an erect growth habit and *S. lautus* native to the rocky headlands have a prostrate growth habit. **c,** Alpine populations of *S. lautus* include a sheltered alpine gully and a wind exposed alpine meadow, containing individuals with an erect and prostrate growth habit, respectively.

Fig. 2: Gravitropism and height variation across 16 *S. lautus* populations.

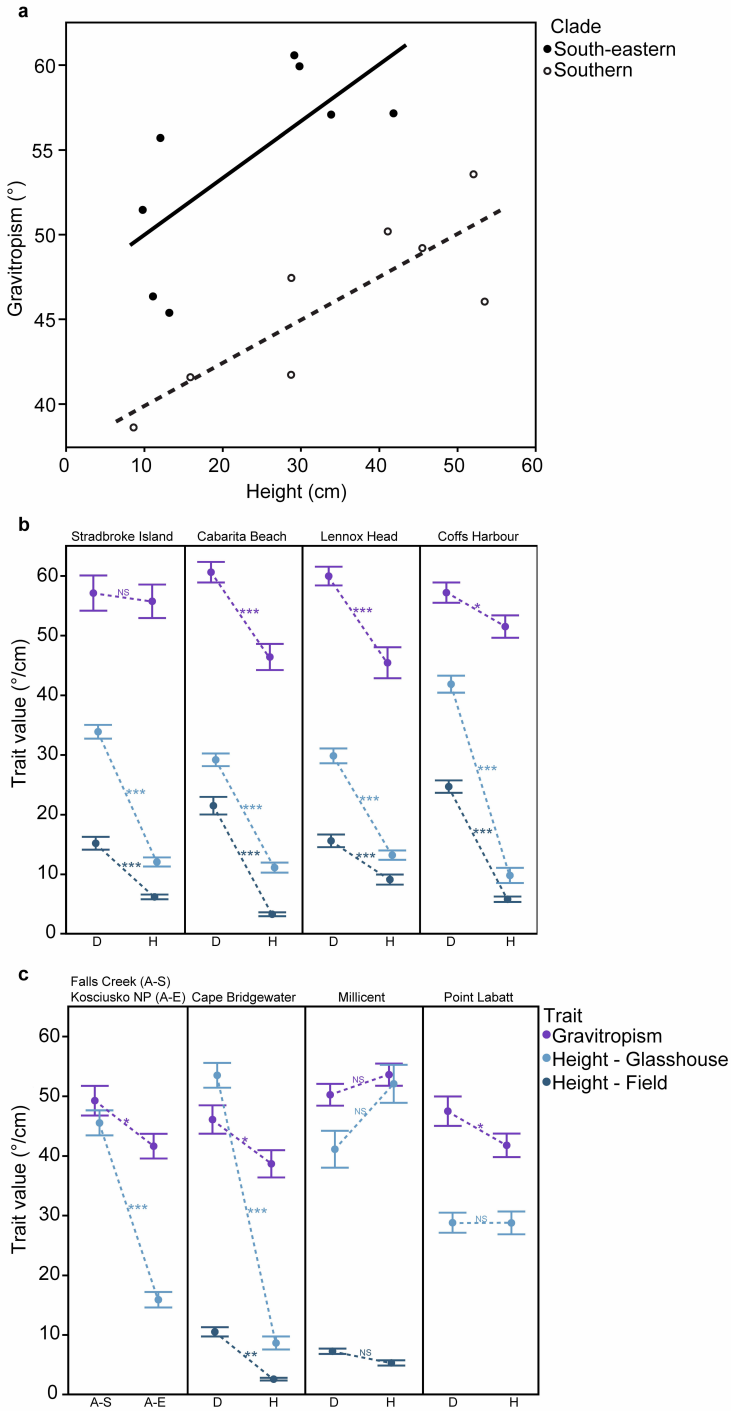

a, The correlation between gravitropism and height across *S. lautus* populations split into their monophyletic clades – see Fig. 1 for details. Each point in the graph represents a population mean where height was measured in the glasshouse and gravitropism was measured 24 hours after a 90° rotation. **b**,**c**, Divergence in gravitropism, height in the glasshouse and height in the field between adjacent *S. lautus* populations (D = Dune, H = Headland, A-S=Alpine Sheltered and A-E = Alpine Exposed). **b**, south-eastern clade and **c**, southern clade. Height in the field for Falls Creek, Kosciusko NP and Point Labatt were not measured. Data are mean ± s.e.m.; one tailed Student's t-test, *P ≤ 0.05, **P ≤ 0.01, ***P ≤ 0.001, NS not significant.

Fig. 3: Parental survival curves in the height (2016) and gravitropism (2012-2014) adaptation experiments at the sand dune and rocky headland at Lennox Head.

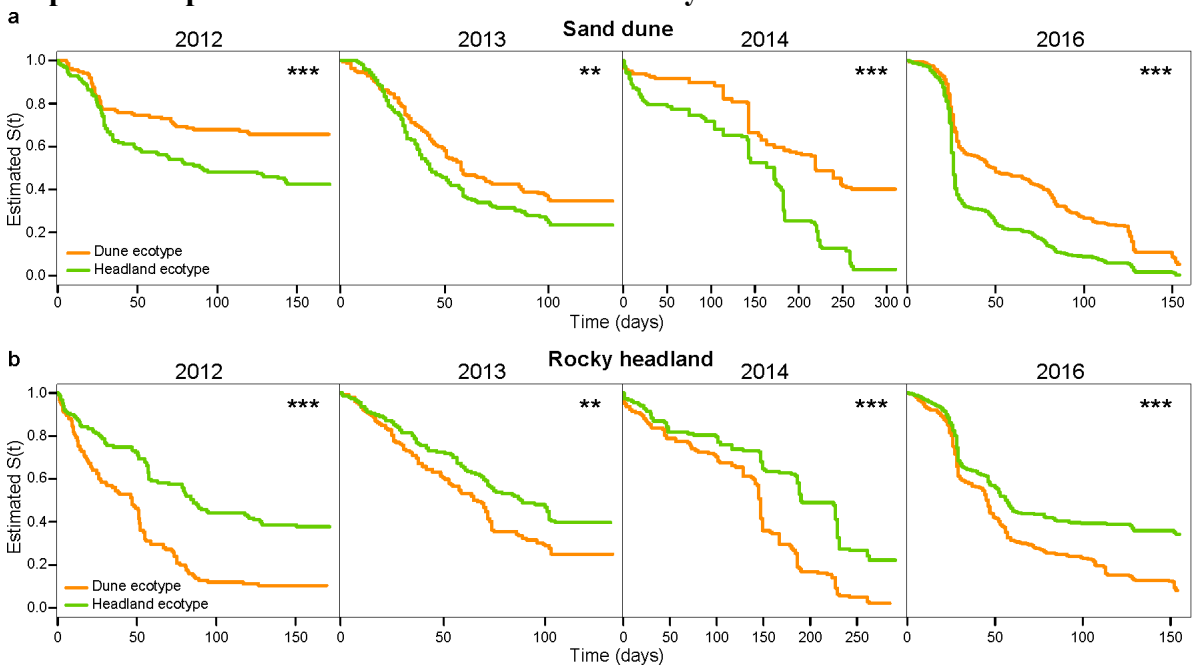

a,**b**, Survival over the length of the field experiments is shown for the Lennox Head Dune population (orange) and the Lenox Head Headland population (green) for four independent field selection experiments at the sand dune (**a**) and rocky headland (**b**). Asterisks indicate a significant difference in mortality risk between the Dune and Headland ecotypes (**$P \leq 0.01$, ***$P \leq 0.001$).

Fig. 4: The creation of the recombinant hybrid generation, the design of the gravitropism adaptation experiments and the measurement of gravitropism.

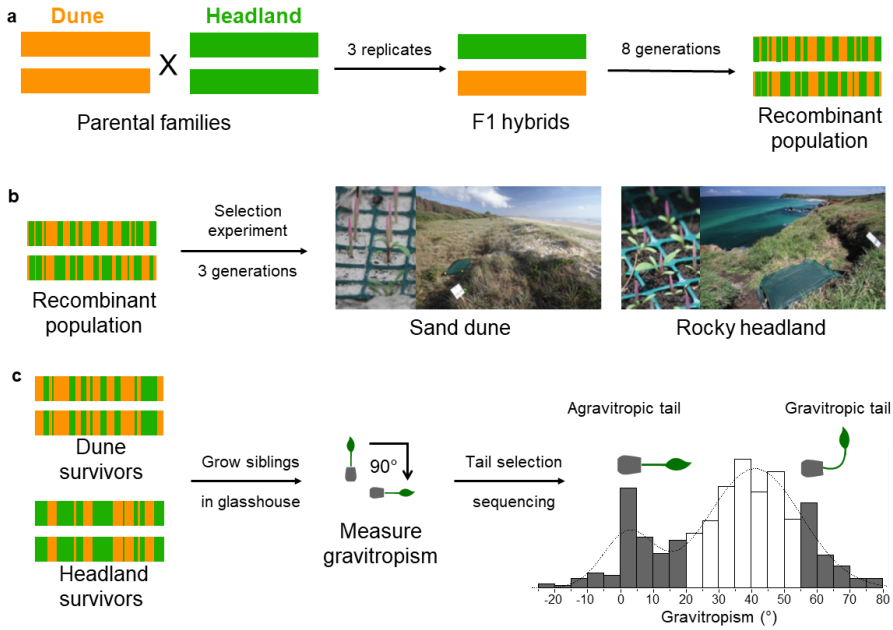

a, A total of 30 parental Dune and Headland individuals from Lennox Head were crossed randomly and with equal contribution for eight generations. **b**, Seeds from this F8 recombinant population were glued to toothpicks and transplanted into the sand dune and rocky headland at Lennox Head. Among-family based selection occurred for three generations (F8, F9 and F10), where full-siblings from the fittest families were grown in the glasshouse and crossed amongst their respective genetic lines (A, B and C) and their environment (Dune survivors or Headland survivors). An inbred control was kept in the glasshouse and underwent the same crossing scheme but free from viability selection. **c**, Gravitropism was measured in the F11 recombinant population by reorientating the plant by 90°. Agravitropic plants have small gravitropic angles, while gravitropic plants have large gravitropic angles as they reorient their growth and grow upright. Individuals in the tails of the gravitropism distribution were sequenced on four lanes of the Illumina HiSeq 4000 platform.

Fig. 5: Association between ENODL1 (early nodulin-like protein 1) and ABA3 (molybdenum cofactor sulfurase) alleles and gravitropism in *S. lautus.*

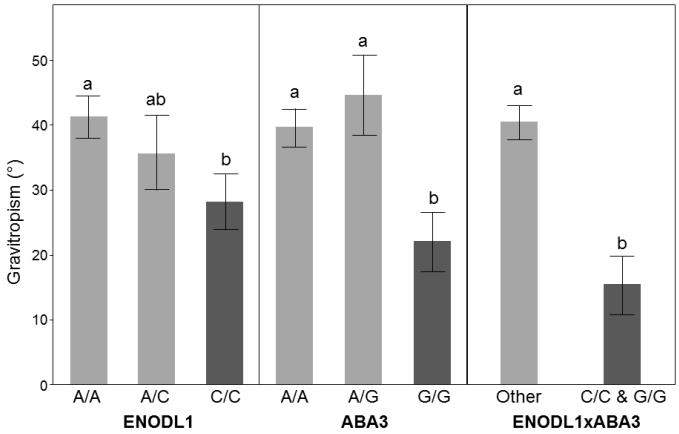

The average gravitropism angle is shown for each allelic combination, independently and when the agravitropic alleles (dark grey) are combined. Different letters denote significant differences between genotypes ($t>1.98$, $p<0.05$).

Methods

Reference genome

Two Lennox Head Headland individuals were used for the creation of the Illumina *S. lautus* reference genome. Firstly, we collected seeds from the Headland at Lennox Head (Extended Data Table 1) and germinated seeds from two individuals by cutting 1mm off the micropyle side of the seed and placing in petri dishes with dampened filter paper. The seeds were placed in darkness for two days for roots to grow and then transferred to 12 hours light/day in a constant temperature room at 25°C for seven days for shoots to grow. Seedlings were then transferred into pots with standard potting mix and grown in the glasshouse. Siblings from the seeds produced were grown and crossed by rubbing flower heads together to produce a family of individuals capable of selfing (rare in *S. lautus*). One generation of selfing was completed to increase homozygosity. We extracted DNA from leaf tissue using the CTAB protocol[55] with column cleaning and overnight incubation. All sequencing was performed by Beijing Genomics Institute (BGI).

A draft genome of *S. lautus* was de novo assembled using second-generation short reads and AllPaths-LG 6.1.2 by utilising a series of eight read libraries (Extended Data Table 2). The reads were trimmed to remove residual adapter sequence and low quality bases (minimum quality 15). The final assembly was ~843MB long and consisted of 96,372 scaffolds with an N50 of 21K. Although 843MB is much shorter than the expected haploid size of 1.38GB[56] of the full genome, the BUSCO gene content completeness of 84% (5% fragmented and 11% missing) suggests that this assembly is primarily missing intergenic repetitive DNA sequences, which are notoriously difficult to assemble. This Illumina assembly was used for mapping of all F11 samples.

A Pacbio *S. lautus* reference genome was then created in an attempt to overcome the problem caused by repetitive DNA. The genome was de novo assembled using next-generation Pacbio long reads and CANU 1.6[57]. A total of 11,481,638 reads (5,072,756 from RSII sequencer and 6,408,882 from Sequel sequencer) were used with a mean read length of ~8K base pairs and an expected genome coverage of ~60x. All sequencing was performed by BGI.

Genetic mapping of convergent traits

Creation of BSA populations

To identify the genomic regions associated to growth habit in *S. lautus*, we created recombinant populations by crossing individuals from four pairs of parapatric populations (Extended Data Fig. 2) that represent independent origins of the erect and prostrate phenotypes[7,9,23,58]. We crossed individuals from contrasting populations growing in the following locations: (1) headland (prostrate) and dune (erect) from Lennox Head (NSW), (2) headland (prostrate) and dune (erect) from Coffs Harbour (NSW), (3) headland (prostrate) and muttonbird island (erect) from Coffs Harbour, and (4) exposed (prostrate) and sheltered (erect) alpine sites from Mt Kosciuszko (NSW) and Falls Creek (VIC), respectively. Using a random-mating-equal-contributions breeding design[59], we crossed multiple individuals from pairs of adjacent populations to create F1s (2 crosses per plant on average) and conducted intercrosses (2 crosses per plant on average) for eight generations between Lennox Head populations (F8-LH), four generations between Alpine populations (F4-A) and three generations between both Coffs Harbour populations (F3-CHD and F3-CHI) (Extended Data Fig. 2).

We measured three phenotypic traits that distinguish erect and prostrate architectures and are possibly regulated by auxins: height, angle of the main stem, and number of tertiary branches.

Height (vegetative) was measured as the vertical distance from the soil to the highest point of the plant that has vegetative leaves (flowers and stems are not included). The angle of the main stem was measured with respect to the soil. Higher values of this angle indicate a more erect stem. To evaluate the number of tertiary branches we collected three basal secondary branches (i.e. branches that originate from the main stem) and counted the number of branches rising from these. Trait distributions and population statistics are provided in Supplementary Table 3.

Genotyping of BSA populations

Genomic DNA of these pools described above was extracted following a modified version of the CTAB protocol[55]. Young leaves were collected and stored at -80°C and ground using a Tissuelyser (Qiagen, Chatsworth, CA). DNA was quantified with the Picogreen reagent (Invitrogen, Carlsbad, CA) and pools of recombinant individuals were created as described in ref. [23]. For each recombinant population we pooled DNA from plants from the 10% tails of the distribution of the three convergent traits (height, angle of the main stem and number of tertiary branches). We thus produced 24 pools of DNA (3 traits x 4 populations x 2 tails; Supplementary Table 4). Pooled DNA was cleaned using the Wizard PCR-cleanup kit (Promega, Sydney, Australia). Libraries of Restriction-site Associated DNA (RAD) tags[60] were created and sequenced at Floragenex (University of Oregon High Throughput Sequencing Facility) following the methodology described in ref. [23] but increasing sequencing depth and coverage (50x depth and 2M reads / sample).

Bulk Segregant Analysis

We identified genomic regions associated to convergent traits by conducting pairwise comparisons between contrasting pools from the same trait and population (3 traits x 4 populations = 12 comparisons). To identify SNPs, determine allelic frequencies and calculate genetic differentiation between pairs of pools, RADseq data was processed using the PoPoolation2 pipeline[61]. Illumina reads were mapped to the PacBio genome draft of *S. lautus* using BWA 0.7.15[62] with default parameters. We then used SAMtools 1.5[63] to create an mpileup file for each pair of pools (Phred quality score of 20). Finally we used the Popoolation2 pipeline 1201[61] to extract variable positions (minimum count of 2, minimum coverage of 15, and maximum coverage of 800), estimate allelic frequency differences[64] between pools and calculate Fisher Exact tests (FET) of allelic differentiation[65-67]. We thus obtained an average number of SNPs per comparison of 39,161 ± 7,244 SNPs located in 10,826 ± 1,405 genomic scaffolds. We called candidate SNPs for each comparison based on two conditions; located in the upper 5 percentiles of the genome-wide distribution of allele frequency differences and having Bonferroni-corrected p-values lower than 5% in the FET. Genomic scaffolds containing at least one candidate SNP were considered candidates for the comparison (Supplementary Table 1 and Supplementary Table 5).

To determine if candidates from BSA of the three traits show footprints of natural selection we re-analysed previous pool-seq samples of natural populations[9,23] and survivors from reciprocal transplants[27] (Supplementary Table 3). We used the pipeline described above to identify candidate SNPs and contigs for pairwise comparisons between adjacent populations[9,23] or survivors from transplants to different environments[27]. To identify SNPs differentiated in natural populations we performed 12 pairwise genomic comparisons between DNA pools from adjacent Dune and Headland populations (Supplementary Table 4).

To identify loci putatively under divergent selection in the sand dune and rocky headland we performed comparisons between pools of survivors from reciprocal transplants using F8 populations (6 comparisons; Supplementary Table 6). Outlier SNPs and scaffolds were defined as described previously for both types of pairwise comparisons.

Differential gene expression between erect and prostrate natural populations

Plant material and RNA extraction

To obtain plant tissue to evaluate gene expression, we used mature plants derived from seeds collected in the field from three erect natural populations: Alpine (A03), Dune (D01), and Tableland (T01), and from one prostrate natural population, Headland (H01). Field-collected seeds were grown under natural light conditions and temperature was controlled to 22°C during the night (6:00pm-6:00am) and 25°C during the day (6:00am-6:00pm). Plants were randomly crossed within each natural population, and 96 seeds of each of the four natural populations were germinated as described above and grown in 48-cell flats in a controlled temperature room at 25°C with a 12-hour light/day cycle. We sampled the shoot apical meristem (SAM) along with the youngest 3 leaf primordia (LP 1, 2 and 3) when plants were 7 weeks old.

cDNA library construction

For each natural population, SAM-LP from each plant was dissected under a dissecting microscope and conserved in RNAlater solution (Ambion, Inc., Austin, USA). Total RNA was extracted using TRIzol[68]. Total RNA was quantified using a NanoDrop (Thermo Fisher Scientific, Waltham, USA) and quality was checked using a bioanalyzer (Agilent technologies, USA) at the Australian Genome Research Facility. Only samples with RNA

integrity number[69] > 6.5 and a ratio of the 28S and 18S ribosomal bands > 1.0 were further processed. 0.5 µg of total RNA were used to construct sequencing libraries with the TruSeq RNA Sample Preparation Kits, and sequenced using 100bp pair-end sequencing with Illumina HiSeqTM 2000 at BGI.

Gene expression quantification

We used the new tuxedo suite, composed of HISAT, StringTie and Ballgown, to identify differentially expressed genes between the prostrate population, H01, and each of the three erect populations, A03, D01 and T01. We first filtered RNAseq raw reads by removing sequencing adaptors, reads with more than 10% unknown bases and more than 50% bases with quality lower than five. Clean reads of each population were mapped to the PacBio *S. lautus* genome draft using HISAT2 2.0.0[70] to align pair-end reads and Samtools 1.5[63] to obtain a sorted BAM files. Stringtie 1.3.4d[71] was used to assemble mapped reads of each population to transcripts, to merge the transcripts of the four populations into a non-redundant set of transcripts contained in the four populations, and to quantify transcript abundances in each of the four populations. Finally, we used the Ballgown[72] R package to obtain the FPKM (fragments per kilobase of exon per million reads mapped) by gene. We calculated the relative expression between erect (A03, D01 and T01) and prostrate (H01) samples as Log2(FPKM erect/ FPKM prostrate; Supplementary Table 7).

Gene annotation

To identify auxin genes associated to the evolution of erect and prostrate phenotypes, we annotated candidate loci from BSA using databases from *Arabidopsis thaliana*, which is the plant model where most studies of auxin signalling have been conducted and has the best

genome annotation among plants. We first conducted a BLASTx of the *S. lautus* genes, as predicted from transcriptome data, against the TAIR protein database (https://www.arabidopsis.org/) using standalone BLAST 2.6.0, and a minimum *e-value* of 1e-6 (Supplementary Table 8). For genomic scaffolds showing associations to adaptive traits in BSA we also searched for genes not detected in the transcriptome by doing a BLATx of the scaffolds against TAIR protein database. We then retrieved the function of significant hits using the DAVID server[73,74] (Supplementary Table 9). Auxin genes were identified by searching for the term "auxin" in this annotation. We refined our functional description of these auxin genes by searching for the terms "biosynthesis", "branch", "efflux", "gravitropism", "influx", "morphogenesis", "polar", "protein modification", "reproduction", "transcription factor", "transport", and "tropism" (Extended Data Table 2). We also searched in the TAIR database for literature references associated to the function of these *Arabidopsis* homologs. Given their large number, these references are not provided in the manuscript.

Phenotyping of natural populations

Height measurements

We measured height as described above in all 16 populations in the glasshouse and 12 of the populations in their native field environment (Supplementary Table 10 and 11). In the field, we measured height in 32 individuals evenly across the range of each population. In the controlled conditions of the glasshouse, we sampled an average of 14 individuals per population after plants reached maturity.

For both the glasshouse and field measurements, we used a linear model to determine whether Dune populations were taller than their adjacent Headland pair: $y_{ijk} = P_i + E_{j(i)} + e_{k(ij)}$, where pair ($P_i$) is an adjacent Dune and Headland population at the same locality and ecotype

($E_{j(i)}$) is Dune or Headland and is nested within pair. All factors are fixed effects and $e_{k(ij)}$ is the residual error. Population height (y_{ijk}) for each pair was compared using a one-tailed t-test. The Alpine populations were also included with the prediction that the sheltered Alpine population (A03) would be taller than the wind exposed Alpine population (A07). All statistical results reported here were produced in JMP 13 (SAS 2015).

Gravitropism measurements

Gravitropism was measured *in vitro* on agar plates in a dark growth cabinet using seeds from all 16 natural populations. For each population, 2-4 seeds per family was grown for ~40 maternal families (1,278 seeds in total). The seeds from a population were combined in a falcon tube and were first sterilised with a quick rinse in 70% EtOH, followed by four 10 minute inversions in a sterilising solution of 6% sodium hypochlorite and 1% Tween 20. Seeds were then rinsed three times with distilled water and vertically orientated on Murashiga and Skoog agar plates containing 0.15% MS, 0.05% MES, 0.15% sucrose and 1% agar. We placed eight seeds on each plate and incubated the plates at 21°C in the dark to avoid any light effects. After seven days, all plates were rotated clockwise by 90° and a photograph of each plate was taken 24 hours after rotation. The photographs were imported into ImageJ[75] to determine gravitropism by measuring the angle to which the stem reorientated to the horizontal[76-78].

Overall there was a 63.8% germination success but we excluded seedlings that were shorter than 5mm, contacted the edge of the plate, or germinated after rotation. This left a total of 736 seedlings across all 16 populations (57.6% of the total number of seeds planted; Supplementary Table 11). To test the hypothesis that Dune populations would have a stronger gravitropic response in their stem than their adjacent Headland pair, we used a mixed linear

model: $y_{ijkl} = P_i + E_{j(i)} + A_k + e_{l(ijk)}$, where pair ($P_i$) is an adjacent Dune and Headland population at the same locality, ecotype ($E_{j(i)}$) is Dune or Headland and is nested within pair, and agar plate (A_k) is the MS plate that the seeds were grown on. Agar plate was fitted as a random effect while the rest were fixed effects, and $e_{l(ijk)}$ is the residual error. Gravitropism measures were averaged for each population and compared between each population pair using a one-tailed t-test. We then tested the correlation between height and gravitropism by performing a linear regression with mean height against mean gravitropism for all 16 populations, where populations were grouped into their respective clades (eastern and south-eastern). All statistical results reported here were produced in JMP 13 (SAS 2015).

Synthetic auxin and auxin transport inhibitor experiments

We tested if gravitropism is governed by auxins in *S. lautus* by evaluating gravitropic responses in seedlings treated with chemicals affecting auxin signalling. Specifically we used 2,4-Dichlorophenoxyacetic acid (2,4-D), a carrier-dependent synthetic auxin[31,79] and Naphthylphthalamic acid (NPA) an efflux inhibitor[32]. We collected seeds from Lennox Head sand dune and rocky headland and grew them on MS containing the different chemicals at concentrations of 0 µM, 0.5 µM, 5 µM and 50µM. For this we used the following stock solutions: 2,4-D: 1mM in Ethanol and NPA: 10mM in DMSO. We created 1ml dilutions of stock solutions (in ethanol or DMSO), which were dissolved in 500 ml of media. Plates were incubated, rotated, photographed and gravitropism was measured in ImageJ[75], as outlined above.

Approximately 40 seeds from different maternal families were planted for each population and chemical concentration. Seeds were excluded from analyses following same procedure above, leaving a total of 188 seedlings to calculate gravitropism. Treatments where few seeds

germinated were excluded (Supplementary Table 12). For each chemical we used a mixed linear model using the lmer function of lme4 package in R v3.1.3[80]: $y_{ijkl} = A_k + E_i + C_j + E_i \times C_j + e_{l(ijk)}$, where agar plate ($A_k$) is the MS plate that the seeds were grown on, ecotype (E_i) is Dune or Headland and concentration (C_j) are the 4 different concentrations of the chemical. Agar plate was fitted as a random effect, while ecotype, concentration and their interaction ($E_i \times C_j$) were fixed effects, and $e_{l(ijk)}$ is the residual error. Gravitropism (y_{ijkl}) was compared using a Type II Wald chi-square test.

Field experiments

All field experiments were conducted at the sand dune and rocky headland at Lennox Head, NSW, in the same location where native *S. lautus* grow. We tracked each individual by gluing each seed to a toothpick and placing 1-2mm under the ground within a grid cell (Fig. 3b) that was randomly assigned (for details see ref. [81] and ref. [21]). 50% shade cloth was initially suspended over all plots to replicate the shade given by surrounding vegetation. Seeds were watered twice a day to keep the soil moist and replicate ideal germination conditions to maximise the number of seeds in the experiment. Once germination plateaued for all genotypes watering was gradually ceased.

Height adaptation experiments

We created genetic lines that aimed to isolate height differences on a common genomic background (Figure 1). Firstly, Lennox Head Dune and Headland seeds were grown and crossed to create an F1 generation. Secondly, to isolate the height alleles on a common genomic background, we introgressed the tall trait onto a headland genomic background by backcrossing the tallest F1 to a Headland parental. This created a BC1F1 generation, where

the tallest individuals (n=11, tallest 20% of the population) were again backcrossed to the Headland parental, creating a BC2F1 generation. We then grew and crossed the tallest BC2F1 individuals (n=18, tallest 10% of the population) among one another and the shortest individuals (n=19, shortest 10% of the population) among one another. These BC2F2 seeds were planted into the rocky headland at Lennox Head on the 2nd October 2016 (Australian spring). We planted five replicate plots, where each plot (1.08x0.33m) consisted of the same 12 families with four (occasionally three) individuals per family in each plot, totalling 843 BC2F2 seeds. The entire field experiment had a total of 4,708 seeds (108 families) but the other genotypes were not relevant to this study. Germination and mortality were recorded every day for 49 days, then every 3-4 days until day 79 and then weekly for the remainder of the experiment (Supplementary Table 13).

We implemented a mixed linear model to test the hypothesis that individuals with short parents will have higher fitness in the headland environment: $y_{ijkl} = H_i + F_j + B_k + e_{l(ijk)}$, where parental height (H_i) was the average height of the parents measured in the glasshouse, family (F_j) was individuals with the same parents, and block (B_k) is the five replicate plots across the rocky headland. Parental height is a fixed effect, and family and block are random effects, and $e_{l(ijk)}$ was the residual error. Offspring fitness (y_{ijk}) was the total number of days alive in the rocky headland from planting. All statistical results reported here were produced in JMP 13 (SAS 2015).

Gravitropism adaptation experiments

We created an advanced recombinant population (F8) from 30 Lennox Head Dune and Headland individuals as described earlier. We replicated the construction of the F8 using three independent replicate crossing lines (A, B and C), all derived from the same base

population. F8 seeds were planted into the sand dune and rocky headlands as described above and the 50% highest surviving families within an environment (and genetic line) were identified, and full-sibling seeds from these families were grown in the glasshouse. To produce the subsequent generations, we used an among-family based selection scheme[82] by conducting crosses among the best surviving families for both the sand dune and rocky headland separately. In crossing the surviving families, we also doubled the crosses per family, ensuring we maintained ~100 full-sibling families for each selection generation planted into the natural environments. Selection was conducted on the F8, F9 and F10 generations.

We selected the top 50% of surviving families in the F8, F9 and F10 field selection experiment using Aster modelling[83,84] implemented with the 'Aster' package in R[80]. The fitness components included germination and survival success, where germination was the total number of individuals that germinated in each family and survival success was the total number of individuals per family that survived to day 85 in the F8 generation, day 138 in the F9 generation, and day 232 in the F10 generation. Finally, to produce the F11 generation, we crossed the F10 generation such that survivors were designated as sires and dams. We then crossed two sires each to two dams in a full-sib, half-sib crossing design.

F11 gravitropism measurements

We measured gravitropism, in the F11 generation described above, as the angle of the stem after a 90° rotation of a seedling (39 Dune families, 37 Headland families and 25 inbred control families with 12 individuals per family (1,212 seeds in total were germinated). The families were germinated in three separate batches ~7 days apart. Briefly, we germinated the F11 seeds by cutting 1mm off the micropyle side of the seed and placing in petri dishes with

dampened filter paper. The seeds were placed in darkness for two days for roots to grow and then transferred to light for 4 days for shoots to grow. Seedlings were then transferred into small square pots with standard potting mix in a constant temperature room at 25°C with a 12 hours light/day cycle. After one week of growing in the pot, the plants were rotated by 90° and a photograph of each individual was taken 12 hours after rotation. The photographs were imported into ImageJ[75] to measure gravitropism as described above. Supplementary Table 14 contains gravitropism measures and dam and sire fitness values.

Gravitropism tests of selection

We implemented a linear model to test the hypothesis that high fitness dune families will produce gravitropic plants and high fitness headland families will produce agravitropic plants. Independent models were used for the sand dune and rocky headland to test the effect of gravitropism on fitness in each environment: $y_{ijklmn} = B_i + V_j + R_{k(i)} + D_{l(ik)} + S_{m(ik)} + e_{n(ijklm)}$, where time-block ($B_i$) is the three time points in which the F11 seeds were grown (~seven days apart); viability (V_j) is the number of days until the death of F11 plants in controlled conditions; and replicate, which consists of the three independent genetic replicates, is nested within time-block ($R_{k(i)}$). Dam fitness was nested in replicate and time-block ($D_{l(ik)}$) and sire fitness was also nested in replicate and time-block ($S_{m(ik)}$). Dam and sire fitness are the F10 family fitness values for the individuals that were crossed to create the F11 offspring where gravitropism was measured. All factors were included as fixed effects and $e_{n(ijklm)}$ was the residual error. Replicate C was removed from analyses as it has little variation in fitness values which means it did not converge. Shapiro-Wilk W test shows the residuals from the model are normally distributed for both the sand dune (W=0.98, p=0.3879) and rocky headland (W=0.98, p=0.2776). The linear model was performed in JMP 13 (SAS 2015).

Genetic association between height and gravitropism

We tested the genetic association between height and gravitropism after segregation in an advanced recombinant population. We implemented a mixed linear model for the three F11 populations (Dune survivors, Headland survivors and a Control population) that accounts for family variation: $y_{ijk} = H_i + F_j + e_{k(ij)}$, where gravitropism ($y_{ij}$) is the angle of the growth response 12 hours after a 90° rotation, height (H_i) is the vertical distance from the soil to the top of the vegetative leaves, measured after maturity in the glasshouse and family (F_j) is a random effect that consists of individuals that have the same dam and sire. The mixed linear model was performed in JMP 13 (SAS 2015).

Genotyping of F11 gravitropism tails

To isolate gravitropism candidate genes we genotyped 77 gravitropic (>56°) and 68 agravitropic (<20°) F11 individuals (Supplementary Table 14). We extracted DNA from leaf tissue using the CTAB protocol[55] with column cleaning and overnight incubation and quantified the DNA using the Picogreen reagent (Invitrogen, Carlsbad, CA). To determine which parent the alleles were derived from, we included 39 Dune parentals (D01) and 41 Headland parentals (H01). Leaves from the Lennox Head Dune and Headland natural populations were collected directly from the field and the same DNA extraction protocol was followed. To increase accuracy of genotyping, each F11 individual was duplicated in independent wells and libraries of Restriction-site Associated DNA (RAD) tags were created at Floragenex following the protocol from ref. [60] but using the PstI restriction enzyme. We sequenced 380 samples on four lanes of an Illumina HiSeq 4000 with 91bp single end reads at Floragenex. A total of 1.39 billion reads with a mean of 3.62 million reads per sample were produced. Reads were aligned to the reference genome using Bowtie 1.1.1[85] and a FASTQ

quality score of above 20. The gravitropism candidate gene set consisted of SNPs in the 99.9% quantile of the distribution of differentiated SNPs between the gravitropism tails. The region of the scaffold containing the SNP was annotated using the blastx NCBI database[86].

Senecio lautus gravitropism candidate genes

In the gravitropism candidate gene set we tested for overrepresentation of gene function and linkage disequilibrium between gravitropism loci. Statistical overrepresentation test was performed in PANTHER (http://pantherdb.org/) using the TAIR identification for 32 unique gravitropism candidate genes matched to a reference list of 27,502 *Arabidopsis thaliana* genes. To calculate linkage disequilibrium between loci, a likelihood-ratio chi-square test was performed in JMP 13 (SAS 2015) with each F11 group independently (Control population, Dune survivors and Headland survivors; Supplementary Table 15).

Intrinsic reproductive isolation

We tested whether intrinsic reproductive isolation was associated with the gravitropism phenotype by randomly crossing within and between the F11 gravitropic and agravitropic groups in a controlled temperature room and recording successful and failed crosses. To maximise sample size, all three replicate genetic lines (A, B and C) were used across all three populations (Dune survivors, Headland survivors and Control). A total of 132 crosses were completed (Supplementary Table 16), 67 crosses between the tails and 65 within the tails (agravitropic tail = 28 and gravitropic tail 37). Crosses were completed by rubbing multiple flower heads of two individuals together and collecting the seeds produced from both plants. To remove genetic incompatibilities that might be caused by relatedness, crosses within the same family were not performed. A failed cross was considered when, in the presence of

pollen, less than three seeds were produced per flower head from both plants with three mating attempts. We performed a two-tailed fisher's exact test in JMP 13 (SAS. 2015) to determine whether there was a significant association between cross type (within vs between gravitropism tails) and failed crosses.

Next, we tested whether intrinsic reproductive isolation was associated with ENDOL1 and ABA3 by calculating the percentage of failed crosses with each allelic combination in the F11 population (Supplementary Table 17 and 18).

55 Clarke, J. D. Cetyltrimethyl ammonium bromide (CTAB) DNA miniprep for plant DNA isolation. *Cold Spring Harbor Protocols* **2009**, pdb.prot5177, doi:10.1101/pdb.prot5177 (2009).

56 Liu, H. *Developing genomic resources for an emerging ecological model species Senecio lautus* PhD Thesis thesis, The University of Queensland, (2015).

57 Koren, S. *et al.* Canu: scalable and accurate long-read assembly via adaptive k-mer weighting and repeat separation. *Genome Res* **27**, 722-736, doi:10.1101/gr.215087.116 (2017).

58 Ali, S. *Senecio lautus* complex in Australia. I. Taxonomic considerations and discussion of some of the related taxa from New Zealand. *Australian Journal of Botany* **12**, 282-291, doi:10.1071/BT9640282 (1964).

59 Rockman, M. V. & Kruglyak, L. Breeding designs for recombinant inbred advanced intercross lines. *Genetics* **179**, 1069-1078, doi:10.1534/genetics.107.083873 (2008).

60 Baird, N. A. *et al.* Rapid SNP discovery and genetic mapping using sequenced RAD markers. *PLOS One* **3**, 1-7, doi:10.1371/journal.pone.0003376 (2008).

61 Kofler, R., Pandey, R. V. & Schlotterer, C. PoPoolation2: identifying differentiation between populations using sequencing of pooled DNA samples (Pool-Seq). *Bioinformatics* **27**, 3435-3436, doi:10.1093/bioinformatics/btr589 (2011).

62 Li, H. & Durbin, R. Fast and accurate short read alignment with Burrows–Wheeler transform. *Bioinformatics* **25**, 1754-1760 (2009).

63 Li, H. *et al.* The sequence alignment/map format and SAMtools. *Bioinformatics* **25**, 2078-2079 (2009).

64 Rosenzweig, B. K., Pease, J. B., Besansky, N. J. & Hahn, M. W. Powerful methods for detecting introgressed regions from population genomic data. *Molecular ecology* **25**, 2387-2397 (2016).

65 Benfey, P. N. & Mitchell-Olds, T. From Genotype to Phenotype: Systems Biology Meets Natural Variation. *Science* **320**, 495-497, doi:10.1126/science.1153716 (2008).

66 Futschik, A. & Schlötterer, C. The Next Generation of Molecular Markers From Massively Parallel Sequencing of Pooled DNA Samples. *Genetics* **186**, 207-218, doi:10.1534/genetics.110.114397 (2010).

67 Magwene, P. M., Willis, J. H. & Kelly, J. K. The statistics of bulk segregant analysis using next generation sequencing. *PLoS Computational Biology* **7**, e1002255, doi:10.1371/journal.pcbi.1002255 (2011).

68 Simms, D., Cizdziel, P. E. & Chomczynski, P. J. F. TRIzol: A new reagent for optimal single-step isolation of RNA. **15**, 532-535 (1993).
69 Schroeder, A. *et al.* The RIN: an RNA integrity number for assigning integrity values to RNA measurements. **7**, 3 (2006).
70 Kim, D., Langmead, B. & Salzberg, S. L. HISAT: a fast spliced aligner with low memory requirements. *Nature methods* **12**, 357-360, doi:10.1038/nmeth.3317 (2015).
71 Pertea, M. *et al.* StringTie enables improved reconstruction of a transcriptome from RNA-seq reads. *Nature biotechnology* **33**, 290-295, doi:10.1038/nbt.3122 (2015).
72 Pertea, M., Kim, D., Pertea, G. M., Leek, J. T. & Salzberg, S. L. Transcript-level expression analysis of RNA-seq experiments with HISAT, StringTie and Ballgown. *Nat Protoc* **11**, 1650-1667, doi:10.1038/nprot.2016.095 (2016).
73 Huang da, W., Sherman, B. T. & Lempicki, R. A. Systematic and integrative analysis of large gene lists using DAVID bioinformatics resources. *Nat Protoc* **4**, 44-57, doi:10.1038/nprot.2008.211 (2009).
74 Huang da, W., Sherman, B. T. & Lempicki, R. A. Bioinformatics enrichment tools: paths toward the comprehensive functional analysis of large gene lists. *Nucleic Acids Res* **37**, 1-13, doi:10.1093/nar/gkn923 (2009).
75 Schneider, C. A., Rasband, W. S. & Eliceiri, K. W. NIH Image to ImageJ: 25 years of image analysis. *Nature Methods* **9**, 671-675 (2012).
76 Sang, D. *et al.* Strigolactones regulate rice tiller angle by attenuating shoot gravitropism through inhibiting auxin biosynthesis. *Proceedings of the National Academy of Sciences* **111**, 11199-11204, doi:10.1073/pnas.1411859111 (2014).
77 Rigo, G. *et al.* Inactivation of plasma membrane-localized CDPK-RELATED KINASE5 decelerates PIN2 exocytosis and root gravitropic response in *Arabidopsis*. *The Plant Cell* **25**, 1592-1608, doi:10.1105/tpc.113.110452 (2013).
78 Rashotte, A. M., Brady, S. R., Reed, R. C., Ante, S. J. & Muday, G. K. Basipetal auxin transport is required for gravitropism in roots of *Arabidopsis*. *Plant Physiology* **122**, 481-490, doi:10.1104/pp.122.2.481 (2000).
79 Yang, Y., Hammes, U. Z., Taylor, C. G., Schachtman, D. P. & Nielsen, E. High-affinity auxin transport by the AUX1 influx carrier protein. *Current Biology* **16**, 1123-1127, doi:10.1016/j.cub.2006.04.029 (2006).
80 Team, R. C. R: A language and environment for statistical computing. *R Foundation for Statistical Computing, Vienna, Austria* (2013).
81 Walter, G. M. *The genetic and ecological basis of diversification* PhD Thesis thesis, The University of Queensland, (2016).
82 Walsh, B. & Lynch, M. *Evolution and Selection of Quantitative Traits: I. Foundations*. (2013).
83 Geyer, C. J., Wagenius, S. & Shaw, R. G. Aster models for life history analysis. *Biometrika* **94**, 415-426 (2007).
84 Shaw, R. G., Geyer, C. J., Wagenius, S., Hangelbroek, H. H. & Etterson, J. R. Unifying life-history analyses for inference of fitness and population growth. *The American Naturalist* **172**, E35-E47, doi:10.1086/588063 (2008).
85 Langmead, B., Trapnell, C., Pop, M. & Salzberg, S. L. Ultrafast and memory-efficient alignment of short DNA sequences to the human genome. *Genome Biology* **10**, R25, doi:10.1186/gb-2009-10-3-r25 (2009).
86 Altschul, S. F., Gish, W., Miller, W., Myers, E. W. & Lipman, D. J. Basic local alignment search tool. *Journal of Molecular Biology* **215**, 403-410, doi:10.1016/s0022-2836(05)80360-2 (1990).

Extended Data Figures and Tables

Extended Data Fig. 1. Repeated divergence in plant architecture traits in *S. lautus* populations.

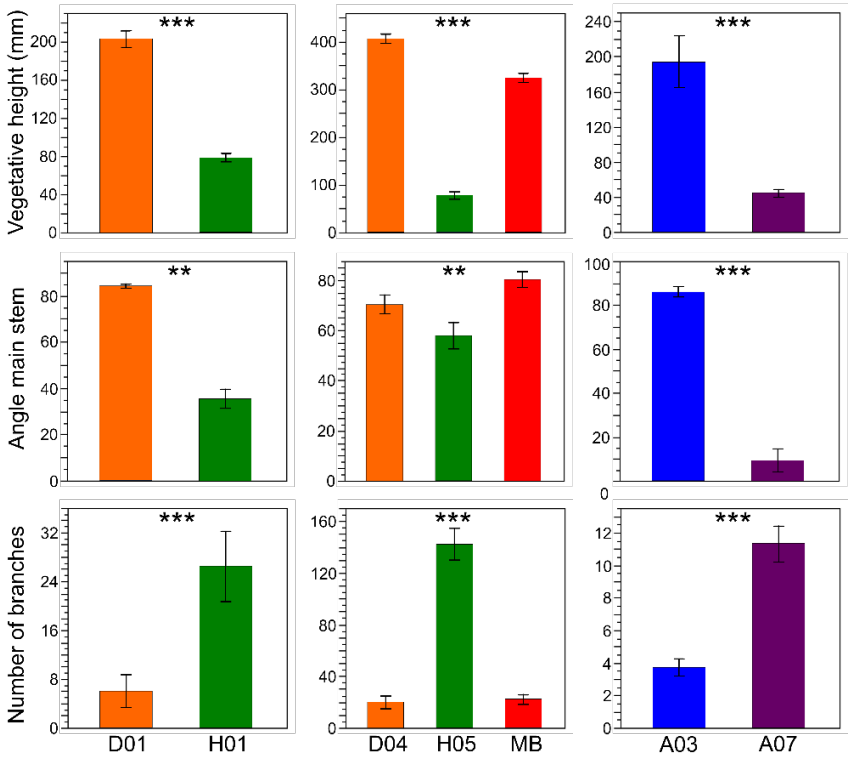

The mean and standard error of three convergent traits in seven natural populations used in this study. For each of the three collection sites we display the results of an ANOVA evaluating the effect of population on mean trait value (**$P \leq 0.01$ and ***$P \leq 0.001$).

Extended Data Fig 2. Genetic mapping of three divergent traits.

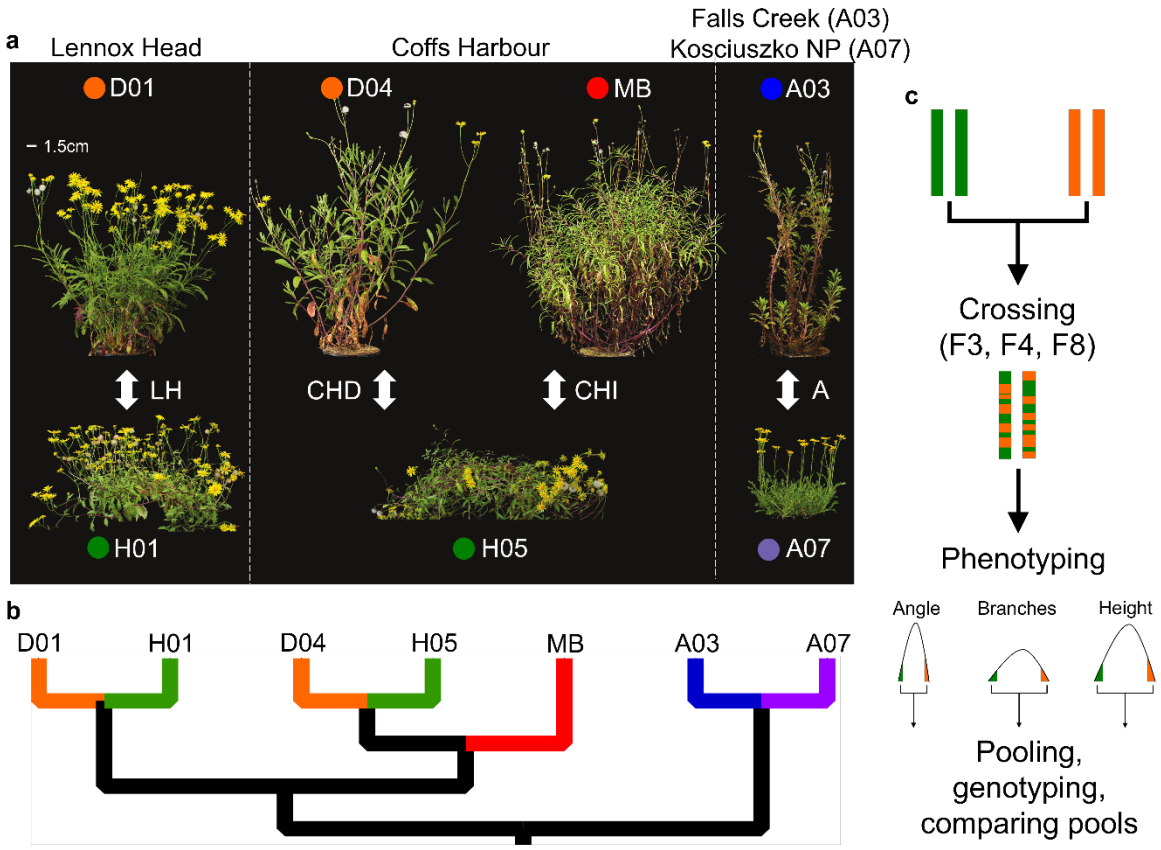

a, Four recombinant mapping populations (LHD, CHD, CHI, A) were created by crossing four pairs of adjacent populations with divergent phenotypes in three locations (Lennox Head, Coffs Harbour and Falls Creek/Kosciuszko NP). Dune populations in orange, headland populations in green and alpine populations in blue (erect) and purple (prostrate). **b**, Phylogenetic relationships between populations as inferred in ref. [23] are shown. **c**, Crosses were conducted between individuals from two adjacent populations to create a recombinant population. In the last generation of inter-crossing the population was phenotyped and the DNA from individuals located in the tails of the distribution of three convergent traits were pooled, genotyped and compared.

Extended Data Fig. 3. Association of auxin genes to three divergent traits.

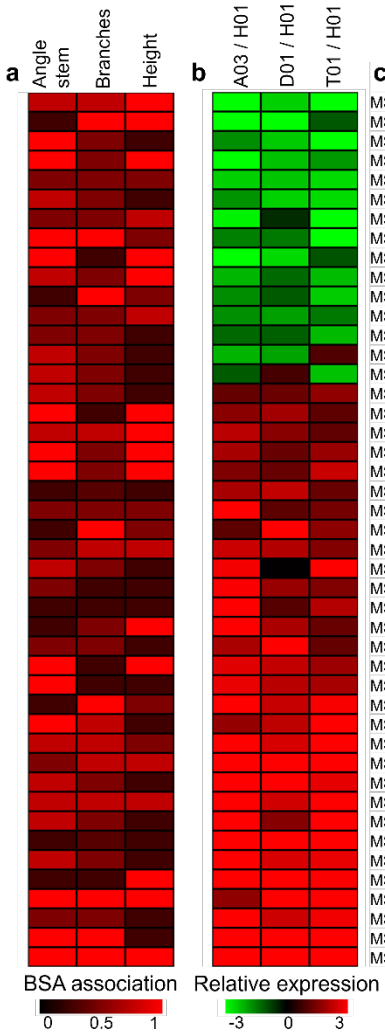

c

Gene	Best hit Tair	Function
MSTRG.1622	AT3G48530	KING1 | SNF1-related protein kinase regulatory subunit gamma 1
MSTRG.53272	AT4G13750	NOV | Histidine kinase-, DNA gyrase B-, and HSP90-like ATPase family protein
MSTRG.19471	AT5G63380	AMP-dependent synthetase and ligase family protein
MSTRG.25245	AT5G13300	SFC, VAN3, AGD3 | ARF GTPase-activating protein
MSTRG.47206	AT5G51190	Integrase-type DNA-binding superfamily protein
MSTRG.49800	AT3G61730	RMF | reduced male fertility
MSTRG.48034	AT1G21410	SKP2A | F-box/RNI-like superfamily protein
MSTRG.62897	AT1G55320	AAE18 | acyl-activating enzyme 18
MSTRG.18674	AT3G55320	PGP20 | P-glycoprotein 20
MSTRG.48658	AT1G78380	ATGSTU19, GST8, GSTU19 | glutathione S-transferase TAU 19
MSTRG.57438	AT4G13750	NOV | Histidine kinase-, DNA gyrase B-, and HSP90-like ATPase family protein
MSTRG.71400	AT3G48530	KING1 | SNF1-related protein kinase regulatory subunit gamma 1
MSTRG.63038	AT3G55960	Haloacid dehalogenase-like hydrolase (HAD) superfamily protein
MSTRG.9642	AT5G67060	HEC1 | basic helix-loop-helix (bHLH) DNA-binding superfamily protein
MSTRG.47189	AT1G48410	AGO1 | Stabilizer of iron transporter SufD / Polynucleotidyl transferase
MSTRG.63000	AT3G10410	SCPL49, CPY | SERINE CARBOXYPEPTIDASE-LIKE 49
MSTRG.64009	AT4G05160	AMP-dependent synthetase and ligase family protein
MSTRG.1625	AT5G50400	ATPAP27, PAP27 | purple acid phosphatase 27
MSTRG.47233	AT4G33090	APM1, ATAPM1 | aminopeptidase M1
MSTRG.11666	AT1G15690	AVP1, ATAVP3, AVP-3, AtVHP1;1 | Inorganic H pyrophosphatase family protein
MSTRG.15707	AT1G48410	AGO1 | Stabilizer of iron transporter SufD / Polynucleotidyl transferase
MSTRG.47203	AT3G26040	HXXXD-type acyl-transferase family protein
MSTRG.21379	AT5G65980	Auxin efflux carrier family protein
MSTRG.50920	AT4G23160	CRK8 | cysteine-rich RLK (RECEPTOR-like protein kinase) 8
MSTRG.9640	AT5G13750	ZIFL1 | zinc induced facilitator-like 1
MSTRG.30734	AT5G03910	ATATH12, ATH12 | ABC2 homolog 12
MSTRG.49760	AT4G13750	NOV | Histidine kinase-, DNA gyrase B-, and HSP90-like ATPase family protein
MSTRG.60235	AT4G33090	APM1, ATAPM1 | aminopeptidase M1
MSTRG.63087	AT2G36985	ROT4, DVL16 | DVL family protein
MSTRG.1836	AT3G62980	TIR1 | F-box/RNI-like superfamily protein
MSTRG.47038	AT1G13570	F-box/RNI-like superfamily protein
MSTRG.46838	AT3G61220	NAD(P)-binding Rossmann-fold superfamily protein
MSTRG.1354	AT1G22380	AtUGT85A3, UGT85A3 | UDP-glucosyl transferase 85A3
MSTRG.47985	AT2G31450	ATNTH1 | DNA glycosylase superfamily protein
MSTRG.50925	AT3G62290	ARFA1E | ADP-ribosylation factor A1E
MSTRG.61257	AT5G36110	CYP716A1 | cytochrome P450, family 716, subfamily A, polypeptide 1
MSTRG.1746	AT2G20760	Clathrin light chain protein
MSTRG.49802	AT2G46520	cellular apoptosis susceptibility protein / importin-alpha re-exporter
MSTRG.32606	AT3G13300	VCS | Transducin/WD40 repeat-like superfamily protein
MSTRG.49801	AT2G46520	cellular apoptosis susceptibility protein / importin-alpha re-exporter
MSTRG.40299	AT3G26810	AFB2 | auxin signaling F-box 2
MSTRG.9024	AT5G65940	CHY1 | beta-hydroxyisobutyryl-CoA hydrolase 1
MSTRG.63071	AT3G46100	ATHRS1, HRS1 | Histidyl-tRNA synthetase 1
MSTRG.35760	AT3G53480	PIS1, PDR9, ATPDR9, ABCG37 | pleiotropic drug resistance 9
MSTRG.63907	AT1G48410	AGO1 | Stabilizer of iron transporter SufD / Polynucleotidyl transferase

a, We show the association of candidate auxin genes (rows) to three traits (columns) in a bulked segregant analysis (BSA). Cell colour indicates the proportion of mapping populations (out of 4) where the gene was associated to the trait. **b**, The relative expression (log2 of the ratio of expression between two samples) between erect (A01, D01, T01) and prostrate (H01) populations. Each column is a comparison between two populations. Genes overexpressed in the erect sample are shown in red. **c**, The gene name, best hit in Tair and the function of each of the genes is shown.

Extended Data Fig. 4. *Senecio lautus* populations in their native environment.

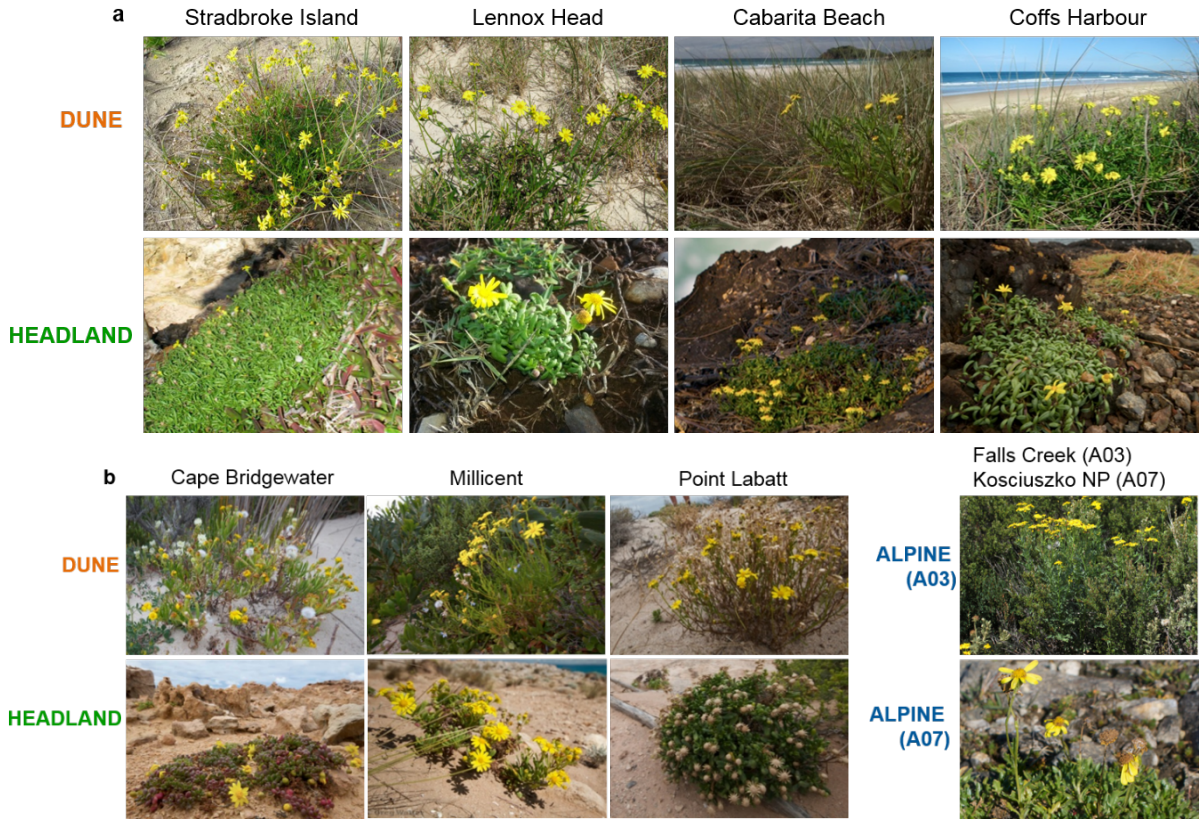

a, The eastern clade where the dune environment is sandy and the plants grow erect, and where the headland environment is rocky and the plants grow prostrate. **b**, The southern clade where the environments are less discrete but in general the Dune plants are erect and the Headland plants are prostrate.

Extended Data Fig. 5. The effect of synthetic auxin (2,4-D) and auxin transport inhibitor (NPA) on gravitropism in plant cells.

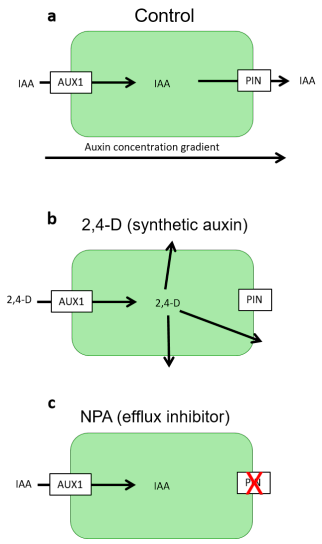

a, When wild type cells (control) respond to a change in the gravity vector, naturally occurring auxin, IAA, enters the cell through AUX1 influx carrier and exits the cell through a PIN efflux carrier. The movement of auxin creates an auxin concentration gradient to initiate bending of the stem. **b**, When synthetic auxin 2,4-Dichlorophenoxyacetic acid (2,4-D) is added, it enters the cell through AUX1 but has low affinity with PIN so diffuses out of the cell, diminishing the ability to create an auxin concentration gradient. **c**, Naphthylphthalamic acid (NPA) efflux inhibitor blocks PIN activity and stops IAA from exiting the cell, also diminishing the formation of an auxin concentration gradient.

Extended Data Fig. 6. The creation of the genetic lines for isolation of growth habit loci.

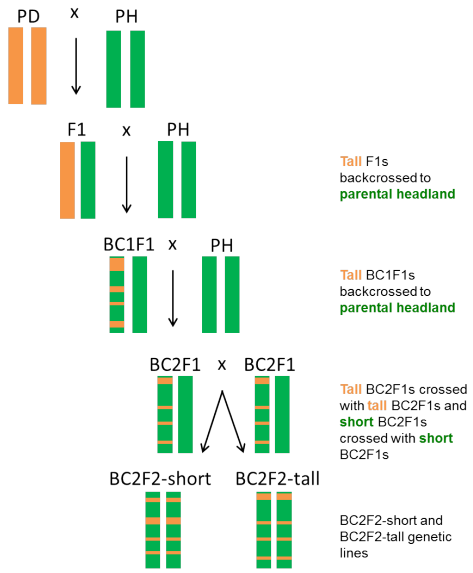

These genetic lines were created by crossing the parental headland (PH) and parental dune (PD) to create an F1 generation containing variation in the erect and prostrate phenotype. Here, we selected the tallest individuals (top 20%) and crossed them to PH. This created a BC1F1 generation (first generation backcross), where the tallest individuals of this generation were again backcrossed to PH, to create a BC2F1 generation. The tallest BC2F1 individuals were then crossed amongst each other (BC2F2-tall) and the shortest BC2F1 individuals were crossed amongst each other (BC2F2-short).

Extended Data Table 1. *Senecio lautus* population pairs and geographic locations.

Clade	Ecotype	Pop	Pop pair	Location	Latitude, longitude
SE	Dune	D00	D00-H00	Stradbroke Island, Flinders Beach*	-27.405604, 153.469734
SE	Headland	H00	D00-H00	Stradbroke Island, Point Lookout	-27.436051, 153.545201
SE	Dune	D03	D03-H02	Cabarita Beach	-28.33179, 153.571379
SE	Headland	H02	D03-H02	Cabarita, Hasting-Point	-28.362477, 153.579662
SE	Dune	D01	D01-H01	Lennox Head, Surf club	-28.787454, 153.593867
SE	Headland	H01	D01-H01	Lennox Head	-28.80607, 153.60275
SE	Dune	D04	D04-H05	Coffs Harbour	-30.312681, 153.140016
SE	Headland	H05	D04-H05	Coffs Harbour, Corambirra Point	-30.311598, 153.143771
S	Alpine	A03	A03-A07	Falls Creek	-36.87236, 147.288594
S	Alpine	A07	A03-A07	Kosciuszko NP	-36.40744, 148.30431
S	Dune	D32	D32-H12	Cape Bridgewater	-38.324472, 141.395222
S	Headland	H12	D32-H12	Cape Bridgewater	-38.376115, 141.366577
S	Dune	D15	D15-H16	Millicent, Canunda National Park	-37.658021, 140.224814
S	Headland	H16	D15-H16	Millicent, Southend, Cape Buffon	-37.565807, 140.108063
S	Dune	D23	D23-H21	Point Labatt, Salmon Beach	-33.125215, 134.265836
S	Headland	H21	D23-H21	Point Labatt	-33.152508, 134.261963

*Different locations were used for D00 seeds in the glasshouse and measurements in the field. The location and GPS coordinates above are for the glasshouse seeds and the field plants were measured at Stradbroke Island, Main beach (-27.51944672, 153.5031086).

The geographic locations of each population used in this study are shown. Populations (Pop) located adjacently to each other have been grouped into population pairs (Pop pair). 'SE' refers to the south-eastern clade and 'S' refers to the southern clade.

Extended Data Table 2. Genomic regions containing auxin genes and displaying strong associations to adaptive traits.

					Footprints of Selection		BSA Number of branches				BSA Angle of the main stem				BSA Vegetative height			
Scaffold ID	Length (bp)	Linkage Group	Auxin genes	Function	Tranplants	Parapatric	CHD	CHI	A	LH	CHD	CHI	A	LH	CHD	CHI	A	LH
tig00001038	221219	GR13	BRL2, CUL1	Pr, Tr	1	2	X		X	X	X	X	X	X				
tig00002103	161587	GR1	BRL2, TIF3H1	Bi, Pr, Tr	1	4	X		X	X	X	X	X	X			X	
tig00002564	207415	GR6	BRL2, CPI1, EXO70A1	Bi, M, Po, Pr, Tr	3	6	X		X	X	X		X	X				
tig00003250	186289		ABCB15	E, G, I, M, Po, Tr, Tp	0	4								X		X	X	X
tig00006349	126098	GR6	TCH2, TCP3, TRN2	Br, M, Tf	1	5					X	X	X					X
tig00011897	45621	GR17	ADS1	E, M, Tr	0	0	X	X	X	X				X				
tig00012479	105485	GR12	NAC6, BIN2, RUB1	Bi, M, Pr, Tf	0	7					X			X				X
tig00015359	94128	GR6	BHLH, HEC1, ZIFL1	G, Po, Tf, Tr, Tp	3	4		X		X	X	X	X					X
tig00019320	65520		BRL2	Pr, Tr	2	4			X	X	X	X				X	X	X
tig00021243	61656		SIP3	Pr, Tr	0	0	X	X	X	X	X							
tig00097475	38773	GR9	AMI1	Bi	2	4	X	X	X					X		X	X	
tig00245460	36177		BRL2	Pr, Tr	0	6		X		X	X	X	X	X				X
tig00245590	220770	GR11	MPK10	M, Pr, Tr	1	1	X	X	X	X				X	X			X
tig00245715	240762		MPK10, MYB16, GN, SIP3	M, Po, Pr, Tf, Tr, Tp	0	5			X	X	X	X	X	X				
tig00245734	291838	GR12	IDD16, AGO1, VPS41	Bi, G, M, Po, Tf, Tr, Tp	1	6		X		X	X	X		X				X
tig00245780	143667	GR1	SPK1	G, Tr, Tp	0	4			X				X			X	X	X
tig00245790	304444		AUF1	Tr	1	4	X		X	X			X		X			
tig00246285	204105	GR1	BRL2	Pr, Tr	0	6		X		X	X	X					X	X
tig00246762	185024	GR5	ABCG37, SAUR70, TAR1	Bi, G, Po, Tr, Tp	1	1	X			X	X	X	X	X			X	
tig00246873	143466	GR1	TT7, CVP2	Bi, Pr, Tr	2	9	X			X			X	X		X		X
tig00247200	168957	GR10	NPY3	Tr	1	5				X		X	X		X			X
tig00247329	120947		Auxin-responsive family protein(AT5G47530)	Tr	0	6		X		X	X	X	X	X				X
tig00247534	161627		TT7, CYP711A1, FLS1	Bi, Po, Tr	0	4			X	X	X		X	X			X	
tig00248540	88423	GR14	NRT1.1	Tr	2	2	X	X	X	X								X
tig00248645	203772	GR14	MPK1, BIN2, WRKY23	M, Pr, Tf, Tr	0	4	X	X		X		X	X		X		X	X
tig00249161	167348		TT7	Bi, Tr	1	1	X	X	X	X								
tig00249185	36537	GR10	BRL2	Pr, Tr	1	2					X				X	X		
tig01928627	312081		SFC, ARF16, ARF8	Bi, G, M, Tf, Tr, Tp	2	0	X			X	X	X	X					X
tig01928645	236709	GR2	ABCB29, ABCB1, TT7, CYP705A22, ABCB2, UGT74D1	Bi, E, G, I, M, Po, Tr, Tp	3	5	X	X				X	X				X	
tig01938487	194373	GR2	TT7, CVP2, 5PTASE13	Bi, G, Pr, Tr, Tp	0	6				X		X				X	X	X
tig01938718	92578	GR8	ABCB11, ABCB21, TOR	E, G, I, M, Po, Tr, Tp	1	1				X		X				X	X	X

For each genomic scaffold identified in the bulk segregant analyses we show the length, the linkage group where it is located[27], the number of putative auxin genes it contains, and the function of the homologs of these genes in *A. thaliana* (see methods, Biosynthesis = Bi; Branch = Br; Efflux = E; Gravitropism = G; Influx = I; Morphogenesis = M; Polar transport = Po; Protein modification = Pr; Reproduction = R; Transcription factor = Tf; Transport = Tr; Tropism = Tp). Footprints of selection were determined using the number of comparisons between pools of survivors where the scaffold shows significant differentiation (total of 6 comparisons) and the number of comparisons between parapatric populations where the scaffold shows significant differentiation (total of 13 comparisons). Association to three convergent traits (number of branches, angle of the main stem, vegetative height) was determined in 4 mapping populations representing independent origins of erect and prostrate architectures (CHD, CHI, A and LH). Scaffolds showing significant association to a trait in a comparison are labelled with an "X".

Extended Data Table 3. The number of seeds and families planted in the sand dune and rocky headland at Lennox Head for each genotype in the F8, F9 and F10 generation in the gravitropism adaptation experiments.

		Sand Dune		Rocky Headland	
Transplant	**Genotype**	**# seeds planted**	**# families**	**# seeds planted**	**# families**
	Parental Dune	180	20	180	20
	Parental Headland	180	20	180	20
2012	**F8-A**	918	34	918	34
	F8-B	702	26	702	26
	F8-C	783	29	783	29
	Parental Dune	180	20	180	20
	Parental Headland	180	20	180	20
2013	**F9-A**	972	36	999	37
	F9-B	783	29	756	28
	F9-C	891	33	891	33
	Parental Dune	180	30	180	30
	Parental Headland	180	30	180	30
2014	**F10-A**	1118	94	1247	94
	F10-B	1023	78	900	78
	F10-C	881	72	882	72
	Total	**9151**	**571**	**9158**	**571**

Parental Dune are Lennox Head native sand dune individuals (D01) and Parental Headland are Lennox Head native rocky headland individuals (H01). A, B and C refers to three independent genetic lines.

Extended Data Table 4. Gene ontology categories overrepresented in the *S. lautus* gravitropism candidate gene set.

GO biological process	N *Arabidopsis* genes	N *Senecio* gravitropism genes	Expected	+/-	*P*
transport (GO:0006810)	2235	11	2.60	4.23	2.67E-05
establishment of localisation (GO:0051234)	2259	11	2.63	4.18	2.95E-05
localisation (GO:0051179)	2345	11	2.73	4.03	4.17E-05
cellular localisation (GO:0051641)	593	8	0.69	11.59	3.26E-07
intracellular transport (GO:0046907)	416	7	0.48	14.46	4.64E-07
establishment of localisation in cell (GO:0051649)	436	7	0.51	13.8	6.33E-07
protein transport (GO:0015031)	606	6	0.71	8.51	6.52E-05
establishment of protein localisation (GO:0045184)	612	6	0.71	8.43	6.88E-05
protein localisation (GO:0008104)	651	6	0.76	7.92	9.63E-05
peptide transport (GO:0015833)	665	6	0.77	7.75	1.08E-04
amide transport (GO:0042886)	674	6	0.78	7.65	1.16E-04
cellular protein localisation (GO:0034613)	408	5	0.47	10.53	1.07E-04
cytosolic transport (GO:0016482)	33	3	0.04	78.13	9.92E-06

PANTHER overrepresentation test was used with *Arabidopsis* thaliana as a reference list (27502 mapped IDs) against 32 *Senecio* gravitropism candidate genes. The *S. lautus* gravitropism candidate gene set consists of loci with the most differentiated SNPs ($\Delta p>0.15$) between gravitropic and agravitropic plants. The number (N) of *Arabidopsis* and *Senecio* gravitropism candidate genes that matched to the overrepresented gene ontology (GO) categories and the expected number of *Senecio* individuals based on the *Arabidopsis* total in each GO category are shown. All GO categories are overrepresented. Transport (GO:0006810) and localisation (GO:0051179) are the parent terms.